

# Responses to Open Discussion Comments

We thank Lutz Gross and both anonymous reviewers for the constructive and thoughtful comments. Addressing them has improved the paper substantially, we think.

Comments are in *blue italic lettering*, responses in black.

## Executive Editor Comments by Lutz Gross

*As explained in [https://www.geoscientific-model-development.net/about/manuscript\\_types.html](https://www.geoscientific-model-development.net/about/manuscript_types.html) it is preferred for the code to be uploaded as a supplement or to be made available at a data repository with an associated DOI (digital object identifier) for the exact model version described in the paper. Given the impermanence of websites, it is not encouraged that authors put models on their own website. Authors should consider improving the availability with a more permanent arrangement.*

Since ARTS is a well-established model, that has been used by its diverse user community for more than 15 years, we prefer to continue to distribute it through the ARTS website.

*On the website [http://www.radiativetransfer.org/misc/download/stable/2.2/several\\_versions/releases](http://www.radiativetransfer.org/misc/download/stable/2.2/several_versions/releases) of the code are available for download. The authors need to explicitly state in the manuscript which version the manuscript is based on and are encouraged to provide the code (possibly as stripped version of the tar-ball) as supplement.*

This is a very good point. The website has been updated to distribute and advertise the exact version that is described in the article, and it also now links directly to the article. The link will be updated after acceptance, of course.

## Reviewer 1 Comments

### *Summary:*

*The article describes the current version of the ARTS package, which is a widely used line-by-line radiative transfer model for the thermal spectral range. The paper is not a complete model description but focuses on new features that have been included after the last ARTS reference publication in 2011. The major extension is a planetary toolbox which enables simulations for the planets Venus, Mars and Jupiter in addition to Earth. The paper is interesting to read, and, as also mentioned in the abstract, it focuses on the major extension, the planetary toolbox, in particular, on how the line-by-line calculations need to be adapted for other planets. My major concern is, that the reader, a potential ARTS user, could think, that this is the main application of ARTS. The introduction summarizes the history of the ARTS development, but afterwards I miss an overview of the features included in ARTS, version 2.2. I think that for example an overview table including the most important ARTS features (not only the new ones) should be added.*

Following this suggestion, we have added a new table to the introduction, summarizing the most important general ARTS features.

*Further it would be nice to include examples of use of the new features, if possible including example input files as supplementary data. The first section should also include something like "basic usage", how the program is installed, how it is executed, etc ...*

We think that kind of information is too technical for the paper. But it is very important, of course. So, motivated by the reviewer comment, we have added a new paragraph in the introduction that describes where this kind of information can be found.

*I have several more specific comments and recommend to publish the paper after the revisions.*

**General Comments:**

*Regarding the planetary toolbox extension, I have general questions: I understood that in detail the absorption lines look different for planetary atmospheres other than Earth because one has to take into account different line broadening parameters and also isotopic ratios are different. It is not clear from the paper how large the resulting differences in the absorption lines actually are.*

We have added a new figure showing the absorption cross-section of the same spectral line for all four different planets, to illustrate the effect of the broadening coefficients. Concerning isotopologue ratios, their impact is better discussed in words, since they simply scale the overall absorption. Such a discussion with numerical examples was also added now.

Additionally, we have added the following comment earlier on: "The consequences of not calculating the broadening correctly can be drastic. In a recent comment, Turbet and Tran (2017) point out that using air instead of the correct CO<sub>2</sub> broadening coefficients may lead to an error of 13 K in the surface temperature in climate simulations for early Mars."

*A further question is, whether it is possible to estimate the error, which would be obtained for broad-band simulations, when the radiance is integrated over a large number of spectral lines. In particular IR instruments often measure broader bands. Does the error for integrated radiance become larger or smaller than for individual lines? Can ARTS without adaptations for other planets be used to simulate IR broad-band observations of other planets?*

The ESA study that funded the planetary toolbox was limited in scope to frequencies up to 3 THz. The separate broadening data for different gases currently therefore is only available for that range. It would be very desirable to extend it through the thermal IR, but this requires funding for a spectroscopy expert to review the available data, as for the lower frequencies.

So, to answer the question: No, with the current ARTS version it is not very meaningful to simulate broad band IR observations for other planets. The broadening parameters for different gases differ systematically, so most likely the differences will not average out for broadband simulations.

*Specific comments:*

*- Abstract: Please motivate, why you have included Faraday rotation and Zeeman splitting.*

*Why are these features needed for atmospheric radiative transfer?*

The paragraph now reads: “Several other new features are also described, notably radio link budgets (including the effect of Faraday rotation that changes the polarisation state), back-scattering radar simulations, and the treatment of Zeeman splitting. The latter is needed in particular to simulate oxygen lines, for example the ones observed by the various operational microwave satellite temperature sensors of the Advanced Microwave Sounding Unit (AMSU) family.”

*p.1, l.16: "computer codes for energy flux computations and remote sensing simulations have been developed in parallel.." - Is this really true? Traditional solution methods like the discrete ordinate method (theory by Chandrasekhar 1950, included e.g. in DISORT code) compute radiance and irradiance simultaneously. I guess that there are more codes that calculate both, e.g. also libRadtran gives radiances, and can also compute (spectrally integrated) irradiances.*

The text was reformulated to make a less strong statement and explain it better: “...From the early days on, high-level computer codes for energy flux computation and remote sensing simulations have developed somewhat independently, and not many complex codes can be used for both applications. Notable exceptions are libRadtran (Emde et al., 2016), which can be used for sensor simulation and flux calculation in the shortwave, and the family of models by AER (Atmospheric and Environmental Research, Clough et al., 2005). The tendency for models to specialise is often not driven by physics (for example low level solvers like DISORT (Stamnes et al., 1988) are suitable for both applications), it rather seems to be driven by practical constraints, resulting from the requirements of the two communities.”

*p.5, Eq. 2: Why has this equation been chosen to calculate the pressure shift in ARTS. Where do the constants 0.25 and 1.5 come from?*

The text was expanded a bit, to read: “The origin of these values for our model is in Pumphrey and Buehler (2000), which in turn refers to Pickett (1980), but that paper, although it does discuss the theory of the pressure shift temperature dependence, does not give any explicit value suggestions for the exponents. Despite its shortcomings, we decided to keep the expression for continuity, and in lack of a better one.”

*Sec. 2.1: Could you include an example plot showing the difference between the two approaches to calculate line broadening and line shift for a spectral line in the Earth atmosphere? How significant is the difference?*

For Earth the practical difference is really small. We have adjusted the text to make this clearer, and added a new paragraph: “However, the practical difference that this makes for Earth is really small. For the example of the 119 GHz oxygen line, the water vapor broadening parameter is roughly 12% larger than the nitrogen broadening parameter (and the oxygen or self- broadening parameter is quite similar to the nitrogen one). Assuming a water vapor VMR of 1% then increases the total width of the line by only about 0.13%. The reason for the small impact is that there is so much more nitrogen and oxygen which dominates the broadening.”

*Here it would also be nice to include ARTS input files (as supplement), showing how to set up the classical absorption calculation and what is changed for the new approach.*

See above. ARTS comes with a large set of example controlfiles, and we now refer to this in the paper. It is in our view better to keep the controlfiles with the code, rather than with the article. It is more user-friendly and easier to maintain in this way.

*p7, l14ff: The line catalogue generated for planetary atmospheres includes data up to 3THz. Are there plans to extend it to the full IR region and possibly also to visible spectral region?*

Not currently, although we would really like to do this. It would require funding for a spectroscopy expert to carefully review the available literature values for the different gases and spectral regions, as for the up to 3 THz region.

Note that HITRAN itself is also moving towards adding separate broadening parameters for different foreign gases, at the moment H<sub>2</sub>, He and CO<sub>2</sub>, as mentioned in the paper at the end of Section 2.2. We plan to adopt ARTS to use these extended HITRAN parameters as they become robustly available.

*p.7 l.21: The sources of data for the planetary database are given in Mendrok et al. 2014. The reference is a technical report for ESA, thus it might be difficult to access it. Please include the data sources in the paper (a table would be nice, perhaps references could be included in Table 2).*

There are a lot of different sources, and also the report describes in detail the rationale for the selection, so we think it really cannot be replaced by a simple table. But we completely agree that it is important that the report is accessible. It is freely downloadable from our web page, but the reference did not include the explicit link, which is now fixed.

*p.11, Sec. 2.3, Refractivity: A plot showing refractive index profiles of all planets in the planetary toolbox would be interesting.*

This has been added now.

*p.11, l. 26. Refer to section 3.1 so that reader knows that radio link simulations are actually possible with ARTS and thus the electron contribution to the refractivity is important to include in the model.*

Done.

*Sec. 2.4: Can you show an example (e.g. a specific water vapor line) and demonstrate how this line changes with different isotopic ratios? I.e. plot the same line for Venus, Earth, Mars and Jupiter.*

We think this is better explained in words than by a figure, since isotopologue abundance simply scales the absorption. The following text has been added to address this comment:

“For spectral lines belonging to molecules that contain heavy hydrogen or nitrogen atoms, the change in absorption due to these abundance differences can be very significant. To give an example, the isotopologue abundance of HDO is more than 100 times that of Earth on Venus, 5 times that of Earth on Mars, and only less than 0.2 that of Earth on Jupiter. Because absorption is proportional to abundance, these differences translate directly into absorption differences for spectral lines belonging to this species.”

*Sec. 2.5: "Doppler shifts" are mentioned here but at this point the reader does not know about this feature in ARTS. Please refer to Sec. 3.3.4.*

Done.

*Sec. 3.1: Please provide one example for a radio link budget simulation.*

A new figure and associated text were added for this.

*p. 14, l. 10: "considers effects covered by geometrical optics ..." - which effects, please describe more precisely. Do you mean Snell's law of refraction or something else? What is meant with "multi-pathing", please explain briefly.*

The text was expanded to hopefully make this clearer: “The most critical step of these calculations is to establish the propagation path between transmitter and receiver. This step is so far only handled by a quite simple and time consuming algorithm (Eriksson et al., 2011c) and only considers effects covered by geometrical optics. Snell's law is used to determine the bending of the radiation as it travels through the atmosphere, and the algorithm looks for a path that connects transmitter and receiver. In reality, there can be more than one possible path for atmospheres with strong vertical temperature gradients (so called multi-pathing), but this is currently not treated in ARTS. The algorithm simply finds a link path, or determines that no path is possible, due to interception by the planet's surface.”

*p. 14, l.15/16: Is it correct that in one of the equations for the "free space loss" the denominator includes  $4\pi$  and in the other  $(4\pi)^2$ ?*

Yes, the definitions are correct, and differ by a factor of  $\lambda/(4\pi)$ . We reformulated the text to make this clearer and added a references for the Friis formula.

*p. 14, l.29: Please explain in a few words what is "Faraday rotation" and why it has to be considered for radio link budget simulations.*

At this place in the text, we just included a reference to the Section where Faraday rotation is discussed. That section was also revised, to hopefully be clearer.

*Sec. 3.2: Please provide one example for a radar simulation.*

In the meantime we have done a lot of work on the radar module in the current development version, and fixed several issues with the implementation in the version that is the subject of the article. We have therefore decided to not advertise the radar

capability of that version, and instead plan to describe it in a separate article, based on the newer implementation. The complete (short) radar section was therefore removed, and also all references to it.

*p. 15, l.9: Please give an example when  $T_h$  and  $T_a$  are not equal. How relevant is this inequality for radar simulations?*

This was in the removed radar part, so it is no longer applicable.

*Sec. 3.1: Please provide an example for non-particle polarization. It would be very interesting to show the circular polarisation by Zeeman splitting. How large is the degree of circular polarisation? For which remote sensing applications is this important?*

The Zeeman effect is discussed in much more depth in the two articles that we cite (Larsson et al. (2014) and Larsson (2014)), including many examples. We prefer to not go into more detail on it here, since we fear that the this aspect is too specialized for the general overview article that this aims to be.

*Sec. 3.3.6: I do not understand this section: Absence of attenuation means vacuum, right? In vacuum there is no refraction. How can the radiance change in absence of attenuation? Please explain.*

Absorption and refraction are different processes, though related. Good optical glass has a high refractivity, but (almost no) absorption.

We now write "This law says that, even in the absence of attenuation, the radiance would change along the propagation path due to refraction effects." Perhaps the "would" makes the meaning a bit clearer.

*p. 19, l.9: The "vacuum speed" is the "speed of light", right?*

Yes. We now write "speed of light in vacuum" to be clear.

*Sec.4. The summary and conclusions section is very short. It should include once more a general overview of what is ARTS, including LBL-absorption calculations, RT in thermal range (microwave, IR), scattering by cloud droplets and (oriented) ice crystals, surface reflection ...*

We think that this repetition would have little added value for the reader, so we prefer to keep the conclusions section very short. It was slightly rewritten, however, to concentrate on the most important points.

## Reviewer 2 Comments

*The Atmospheric Radiative Transfer Simulator (ARTS) is a versatile radiative transfer tool (apparently) mainly oriented towards various remote sensing applications. The paper by Buehler et al. describes version 2.2 of ARTS, with emphasis on new features not present in previous versions. A documentation of ARTS in an open-access journal like GMD would be very welcome, especially as the two peer-reviewed publications describing earlier versions*

of ARTS as a whole (Buehler et al. (2005a), Eriksson et al. (2011a); papers cited in the manuscript) have been published in JQSRT — which is a respectable journal but not accessible to everyone (including me, as an employee of a national weather service with a very large research department).

While I think it would be important to publish this work, I also think that this paper is clearly in need of improvement. Suggestions for improvement are given below.

### **Major comments**

1. The focus on new features of ARTS is certainly a deliberate choice by the authors, but in my opinion it does not work entirely satisfactorily, at least for readers who are not familiar with ARTS beforehand. Much of the discussion is focused on how to compute gaseous line absorption parameters for planets with differing gaseous composition, and on exotic effects like Faraday rotation and Zeeman effect. However, the basic features of ARTS are not described properly (if at all), so the most basic question remains unanswered: What is ARTS and what can it be used for?

Therefore, I strongly recommend adding a section that summarizes the basic features of ARTS, not only the new features.

The introduction was extended with a brief discussion of general ARTS features, including a feature table, as suggested by the reviewer below.

*The list of issues that should be reported includes at least the following:*

- *How is the radiative transfer equation solved: (i) scalar or vector radiative transfer; (ii) methods of treating multiple scattering; (iii) solution geometry?*

Done (in table).

- *What is the wavelength region (that can be) considered?*

Done (in table).

- *Treatment of gaseous absorption: (i) basic method (line-by-line?), (ii) absorbing species (you could possibly refer to Table 2); (iii) sources of line data?*

Done (in table).

- *Treatment of emission (Planck function, local thermodynamic equilibrium)*

Done (in table).

- *Treatment of scattering and absorption by particles (e.g., those in clouds)? E.g., what are the choices available for particle single-scattering properties?*

Done (in table).

- *Treatment of the surface?*

Done (in table).

*I recognize that some of this information is provided in the Introduction and in other sections, but it should be provided in a more coherent and systematic manner. It is not*

*necessary to discuss all these features in-depth (most of the information could probably be put in a table), but the basic information should be provided, to put the new features in the context.*

We like the suggestion of a feature table, and this is the way we have implemented the general overview now.

*2. An unusual feature of this article is that it contains no results and almost no figures. While this is, of course, related to the nature of the article as a model description paper, it makes the paper rather boring to read. Some practical examples would be helpful. A couple of possibilities (you are welcome to invent more examples yourselves):*

Following the suggestion, we have added five new figures to the paper now.

- In Sect. 2.1, show some examples of how different gas composition for different planets influences, through line broadening, the absorption spectrum of selected gases (e.g., CO<sub>2</sub> absorption on Earth vs. Mars).*

Done, we show the effect of planetary composition on the broadening of an H<sub>2</sub>O line in a new figure.

- In Sect. 3.3.3, show an example of how the Zeeman effect splits a spectral line into several lines. I would be curious to see if this effect is relevant, for example, for Earth's middle/upper atmosphere.*

The Zeeman splitting is discussed at length and with figures in the cited articles, so we do not want to duplicate that here. The effect is important on Earth for example for high-altitude AMSU-A temperature sounding channels (in the 60 GHz O<sub>2</sub> line cluster).

*3. The paper provides no information on if and how users of ARTS can verify whether they are using the model correctly. An ideal solution would be to provide a selection of test cases against which the users can compare their results. If this is impractical in the context of this paper (e.g. considering the length of the paper), it would at least be worth mentioning whether such test cases are provided at [www.radiativetransfer.org](http://www.radiativetransfer.org), where ARTS is available.*

We have indeed such a mechanism. The following text has been added in the introduction to describe it: "..., the distribution includes a large set of sample controlfiles for ARTS that contain predefined setups for various remote sensing instruments, and demonstration cases for various ARTS features. There also is a build target 'make check' that runs a selection of the included controlfiles and compares their computation results against reference data. For the user, this allows to verify that the model works correctly. For the developers, perhaps even more importantly, it helps to ensure continuity and prevents unintentional changes in model output due to source code changes."

### **Minor comments**

*1. p. 5, l. 10: How large are the pressure-dependent frequency shifts typically, e.g. at the surface level on Earth?*

For the 183 GHz H<sub>2</sub>O line, the “air” shift parameter is -891 Hz/Pa, so at 1000 hPa the shift is almost 90 MHz. Due to the strong broadening, the line center is hard to observe directly at these high pressures, so the main effect of the shift is that it make the line asymmetric.

*2. p. 5, Eq. (2): In the exponent, should nair be na?*

Yes, thanks for spotting the typo.

*Also, how did you choose the constants 0.25 and 1.5 (you state below Eq. (2) that this equation comes without any claim of general validity, but probably these are not totally arbitrary either)?*

We added a bit more explanatory text. There really is only a very poor basis for these constants, and we have now formulated this more strongly. We just use them for lack of better ones.

*3. p. 7, l. 15: What is the wavelength range supported by ARTS? It is said here “up to 3 Thz”, which corresponds to 100 μm, but ARTS has also been used for computing radiative fluxes integrated over the thermal infrared region (which starts at about 4 μm) (Pincus et al. 2015, paper cited in the manuscript). Is it so that the ARTS spectroscopic database starts at 100 μm and other databases (=HITRAN?) have to be used at shorter wavelengths? Please clarify.*

Yes, it is only the new planetary line database that is limited to frequencies below 3 THz. This is now stated explicitly in the feature table.

*4. p. 7, l. 29: “...Explicit values have been put where available”. It is not obvious what this means. “Directly measured values”?*

The term explicit was misleading. The paragraph was reformulated, to now read: “Foreign species specific line parameters have been derived by a careful literature investigation searching for experimental or theoretical studies specifically devoted to line broadening and shift by He, H<sub>2</sub>, CO<sub>2</sub>, or H<sub>2</sub>. Furthermore, air broadening and shift parameters reported in the HITRAN database are often deduced from individually determined and reported N<sub>2</sub> and O<sub>2</sub> broadening and shift data. In such cases, we applied the original N<sub>2</sub> and O<sub>2</sub> literature data in our catalogue compilation. For some combinations of gas species, absorption line and perturbing gas, the broadening and line shift parameters are absent in the literature, simply because spectroscopic studies dealing with these line parameters were never performed. In this case, the values quoted in our catalogue have been reasonably estimated, where the estimation strategy could differ from one absorption species to the other.”

*5. p. 9, Table 2: This lacks some gases (most notably CFCs) relevant for climate change. Is it because of the wavelength range considered?*

CFCs (and in general gases that are included in HITRAN only as absorption cross section data, not line parameters) are missing in the ARTS version described. We are working on adding them in the current development version, and also plan a short article about it.

6. p. 21, l. 11–12: Mention that CO2 line mixing is already available in ARTS2.3? Pincus et al. (2015) (paper cited in the manuscript) discuss this explicitly.

We want to avoid too many references to the current development version. Mostly because we want to thoroughly test these new features before they are advertised too widely.

*Technical corrections*

1. p. 2, l. 1: replace “inside” with “among”

Done.

2. p. 3, l. 29: replace “triggered” with “motivated”?

Done.

3. p. 9, l. 12–13: this should be “dependence ... on”

Done.

4. p. 11, l. 10: this should be “Earth’s”

Done.

5. p. 11, l. 17: replace “sumbillimeter” with “submillimeter”

Done. (Although we actually like the term “sumbillimeter”)

6. p. 15, l. 2: replace “underestimation” with “underestimate”

This section has been removed now.

7. p. 18, l. 27: this should be “frequency-dependent”

Done.

8. p. 19, l. 27: this should be “variety”

Done.

9. p. 20, l. 2: this should be “seamlessly”

Done.

10. p. 26, l. 2: The length of Larson (2014) is probably less than 1009 pages.

Corrected (and also added missing DOI number).

# ARTS, the atmospheric radiative transfer simulator — version 2.2, the planetary toolbox edition

Stefan A. Buehler<sup>1</sup>, Jana Mendrok<sup>2</sup>, Patrick Eriksson<sup>2</sup>, Agnès Perrin<sup>4</sup>, Richard Larsson<sup>5</sup>, and Oliver Lemke<sup>1</sup>

<sup>1</sup>Meteorologisches Institut, Centrum für Erdsystem- und Nachhaltigkeitsforschung (CEN), Fachbereich Geowissenschaften, Fakultät für Mathematik, Informatik und Naturwissenschaften, Universität Hamburg, Bundesstrasse 55, 20146 Hamburg, Germany

<sup>2</sup>Department of Space, Earth and Environment, Chalmers University of Technology, SE-41296 Gothenburg, Sweden

<sup>4</sup>Laboratoire de Météorologie Dynamique/IPSL, UMR CNRS 8539, Ecole Polytechnique, Université Paris-Saclay, RD36, 91128 PALAISEAU Cedex, France

<sup>5</sup>National Institute of Information and Communications Technology, 4 Chome-2-1 Nukui Kitamachi, Koganei, Tokyo JP-184-0015, Japan

*Correspondence to:* S. A. Buehler (stefan.buehler@uni-hamburg.de)

**Abstract.** This article describes the latest stable release (version 2.2) of the Atmospheric Radiative Transfer Simulator (ARTS), a public domain software for radiative transfer simulations in the thermal spectral range (microwave to infrared). The main feature of this release is a planetary toolbox, that allows simulations for the planets Venus, Mars, and Jupiter, in addition to Earth. This required considerable model adaptations, most notably in the area of gaseous absorption calculations. ~~Several~~ 5 ~~other~~ Other new features are also described, notably radio link budgets ~~, back-scattering radar simulations, and the treatment (including the effect~~ of Faraday rotation ~~and Zeeman splitting, that changes the polarisation state), and the treatment of Zeeman splitting for oxygen spectral lines. The latter is for example relevant for the various operational microwave satellite temperature sensors of the Advanced Microwave Sounding Unit (AMSU) family.~~

## 1 Introduction

10 Numerical radiative transfer (RT) modeling with computers perhaps started from the urge to understand atmospheric radiant energy fluxes. The earliest general circulation model (Phillips, 1956) did not yet include a radiation scheme, but simply assumed a globally constant radiative heating rate. In the same year, Plass (1956) already published an article describing numerical simulations of infrared radiation. This paved the way for simple one-dimensional radiative convective models of Earth's energy balance (Manabe and Möller, 1961), and later for global circulation models with sophisticated radiation schemes. It is fair to say 15 that numerical radiative transfer simulations started as soon as computers were becoming available to atmospheric scientists. Since then, the atmospheric sciences have had a constant need for ever more accurate and efficient RT simulation software.

Besides radiative energy flux calculation, the other important application area for RT software is remote sensing. This started almost at the same time as the energy flux simulations, an early example is Kaplan (1959). From the early days on, high-level computer codes for energy flux computation and remote sensing simulations have developed ~~in parallel, but nearly~~

somewhat independently, and ~~few-not many complex~~ codes can be used for both applications. ~~A notable exception is the~~ Notable exceptions are libRadtran (Emde et al., 2016), which can be used for sensor simulation and flux calculation in the shortwave, and the family of models by AER (Atmospheric and Environmental Research, Clough et al., 2005). The tendency for models to specialise is often not driven by physics (for example low level solvers like DISORT (Stamnes et al., 1988) are  
5 suitable for both applications), it rather seems to be driven by practical constraints, resulting from the requirements of the two communities.

A similar partitioning exists even ~~inside-among~~ the remote sensing RT codes themselves. Historically, most codes were developed for a particular sensor, or remote sensing technique, so that there are dedicated codes for active or passive sensors, microwave, infrared, or ultraviolet/visible frequencies, and up-looking, down-looking, or limb-looking geometry. Moreover,  
10 such partitioning also exists regarding the object of observation like the different bodies of the solar system.

Radiative transfer models for planets other than Earth have been developed about equally as long as ~~such~~ for Earth itself (e.g., Cess, 1971). Also, terrestrial radiative transfer codes have frequently been used to simulate spectra of solar system as well as exo-planets with certain modifications or extensions of, e.g., the spectroscopic data applied (~~e.g. Urban et al., 2005; Bernstein et al., 2007; K~~  
15 ~~e.g. Urban et al., 2005; Bernstein et al., 2007; Kasai et al., 2012; Vasquez et al., 2013a, b; Schreier et al., 2014~~). Few have been explicitly developed with a view on applicability to a wide range of different planet characteristics, ~~i.e. to be able to treat very different basic composition of the atmospheres, wide ranges of atmospheric temperatures, etc.,~~ like e.g., VSTAR (Versatile Software for Transfer of Atmospheric Radiation, Bailey and Kedziora-Chudczer, 2012) or SMART (Spectral Mapping Atmospheric Radiative T  
20 . Interest in prediction and analysis of non-Earth spectra has increased significantly in recent years in relation with due to intensified research into habitability of planets and the search for exoplanets, calling also for more consistent and more generally applicable models.

Regarding Earth observations, the separate development of models for spectral regions or measurement techniques now proves to be an obstacle for synergistic use of modern multi-sensor observations, which requires consistency in the simulation of all involved sensors. Out of an appreciation of this, a few RT codes have been developed that are fairly broad in scope, agnostic of a particular sensor, and used for a wide range of applications. Besides the already mentioned AER model family, ~~libRadtran~~  
25 ~~(Emde et al., 2016)(Clough et al., 2005) and libRadtran (Emde et al., 2016), Dudhia (2017) and Schreier et al. (2014)~~ could be named here as ~~a multi-purpose model toolbox for the visible and infrared spectral range, as well as Dudhia (2017) and Schreier et al. (2014) as~~ general-purpose models for the infrared spectral range; and of course the Atmospheric Radiative Transfer Simulator (ARTS), the subject of this article.

The ARTS project started in the year 2000 as a joint initiative of Patrick Eriksson (Chalmers) and Stefan Buehler (then  
30 at University of Bremen). Table 1 presents a very brief summary of general ARTS features. Right from the start the code was open source (GNU's Not Unix (GNU) public license); the current version is freely available at [www.radiativetransfer.org](http://www.radiativetransfer.org). At the start, the model focused on simulating clear-sky limb observations of Earth's atmosphere in the millimeter and sub-millimeter spectral range, because that was the main interest of the authors (Eriksson et al., 2002; Buehler et al., 2005b). Pretty soon, the interests widened, and ARTS adopted new capabilities such as simulating downlooking meteorological microwave  
35 sensors (Buehler et al., 2004; John and Buehler, 2004) and active radio link measurements (Eriksson et al., 2003). ARTS was

also started to be used for infrared energy flux simulations (Buehler et al., 2006b; John et al., 2006), and the capability to handle cases with scattering by hydrometeors was developed by two different scattering solvers, the discrete ordinate iterative solver (DOIT, Emde et al., 2004a, b), employed for example in Rydberg et al. (2007) and Sreerekha et al. (2008), and a Monte Carlo solver (MC, Davis et al., 2005, 2007), for example used in Rydberg et al. (2009) and Eriksson et al. (2011d).

5 ARTS comes with a quite complete set of documentation, consisting of four main elements: First, the top level directory of the distribution contains several readme files that describe the program configuration, compilation, and execution. Command line options are also explained by the program itself when run with the '-h' or '-help' command line option. Configuration and compilation follow standard open source unix programming conventions. Second, there are the guide books (User Guide, Theory Guide, and Developer Guide), which give a comprehensive overview of the program from a user perspective, from a  
10 theoretical perspective, and from a programming perspective, respectively. Third, ARTS works like a scripting language with functions (in ARTS called *methods*) that work on variables (in ARTS called *workspace variables*), and each of these functions and variables has built-in documentation, perhaps comparable to a Unix man page, that can be browsed online at the ARTS website. Fourth, the distribution includes a large set of sample *controlfiles* for ARTS that contain predefined setups for various remote sensing instruments, and demonstration cases for various ARTS features. There also is a build target 'make check' that  
15 runs a selection of the included controlfiles and compares their computation results against reference data. For the user, this allows to verify that the model works correctly. For the developer, perhaps even more importantly, it helps to ensure continuity and prevents unintentional changes in model output due to source code changes.

Over the years, the model was validated by several inter-comparison studies ~~for example by Melsheimer et al. (2005) and Buehler et al. (2006a). Most~~ (e.g., Melsheimer et al., 2005; Buehler et al., 2006a; Schreier et al., 2018). Quite recently, the  
20 ARTS infrared energy flux calculations were used as one of the reference models in a broad assessment of the quality of radiation codes in climate models (Pincus et al., 2015), and were shown to be in very good agreement with the other participating reference models. Also, closure studies with radiosondes, microwave observations, and infrared observations increase our confidence that the model consistently handles the different spectral ranges (~~Kottayil et al., 2012~~)(Kottayil et al., 2012; Bobryshev et al., 2018)

25 Perhaps the most significant limitation, though, that remains even to date, is that ARTS does not have a collimated beam source, so it currently cannot simulate solar radiation observations or solar radiation energy fluxes. The line-by-line absorption calculation itself, however, does work also in the solar spectral range, and has been used by Gasteiger et al. (2014) to precalculate absorption cross sections for libRadtran (Emde et al., 2016), using the simulated annealing method described in (~~Buehler et al., 2010~~)Buehler et al. (2010).

30 There are only two previous publications that describe earlier versions of ARTS as a whole, Buehler et al. (2005a) and Eriksson et al. (2011a), but many of the main building blocks of ARTS and the tools around it have been described in dedicated publications. Besides the already mentioned DOIT and MC scattering solvers, important building blocks are the method to pre-calculate and store gas absorption data (Buehler et al., 2011) and the method to handle sensor characteristics by building up a comprehensive sparse matrix sensor representation (Eriksson et al., 2006).

**Table 1.** An overview of general ARTS features.

---

<u>Name</u>	<u>Atmospheric Radiative Transfer Simulator (ARTS)</u>
<u>Website</u>	<u>radiativetransfer.org</u>
<u>Programming language</u>	<u>C++ (with accompanying tools in Python and Matlab)</u>
<u>Flow control</u>	<u>Scripting-language-like controlfiles allow large flexibility in calculation setup</u>
<u>Input and output file formats</u>	<u>XML, NetCDF, some specialised formats for spectroscopic data (e.g., HITRAN)</u>
<u>License</u>	<u>GNU Public License</u>
<u>Absorption calculation types</u>	<u>Line-by-line or lookup table (absorbing species see Table 4)</u>
<u>Spectral range for absorption calculation</u>	<u>Microwave to visible</u>
<u>Spectroscopic data</u>	<u>Data up to 3 THz are included for Earth, Venus, Mars, and Jupiter; standard databases (e.g., HITRAN) can be used at higher frequencies</u>
<u>Continuum absorption</u>	<u>Built-in continuum absorption models for microwave to infrared (but not visible)</u>
<u>Radiative transfer calculation type</u>	<u>Solves monochromatic pencil beam radiative transfer equation with thermal emission and optional scattering, pure transmission calculation also possible</u>
<u>Source function</u>	<u>Planck function or pure extinction (using physical temperature as source function for Rayleigh-Jeans limit calculations also works, but is not recommended)</u>
<u>Spectral range for radiative transfer simulation</u>	<u>Microwave to thermal infrared (no collimated beam solar source)</u>
<u>Viewing geometries</u>	<u>Up-looking, down-looking, limb-looking, sensor inside or outside the atmosphere</u>
<u>Model geometry</u>	<u>Spherical 1D, 2D, or 3D (with plane parallel as limiting case for large planet radius)</u>
<u>Polarisation</u>	<u>Scalar intensity, selected Stokes components, or full Stokes vector</u>
<u>Surface roughness</u>	<u>Specular reflection or arbitrary reflection pattern</u>
<u>Surface topography</u>	<u>Allowed for 2D and 3D geometry, none for 1D by definition</u>
<u>Passive sensors</u>	<u>Comprehensive linearised sensor treatment for efficient weighting of monochromatic pencil beam radiances</u>
<u>Active sensors</u>	<u>Radio occultation (intensity only, no wave propagation)</u>
<u>Scattering solvers</u>	<u>Discrete Ordinate Iterative (DOIT) solver; Monte Carlo (MC) solver (for the stable version described in this article, the development version includes several additional solvers)</u>

Important tools around ARTS are the Qpack Matlab package (Eriksson et al., 2005) that, among many other things, allows optimal estimation inversions (going from measured or simulated radiation back to an estimate of the atmospheric state), and a Matlab package for frequency grid optimisation by simulated annealing (Buehler et al., 2010), which both are part of the bigger Matlab package ATMLAB (ATMospheric matLAB), freely available from the ARTS website. The website also holds arts-xml-data, a data package with model atmospheres, spectroscopic data, and other data that are required or useful for running radiative transfer simulations. And, last but not least, there is a growing set of Python interface and helper functions, collected in a package called Typhon.

This article describes ARTS version 2.2. The most visible difference to prior versions is that the program, originally developed for Earth, has been adapted to also work well for the other solar system planets, specifically Mars, Venus, and Jupiter. These additions were developed in a study supported by the European Space Agency (ESA). Along with the program itself comes a set of inputs for the different planets, such as spectroscopic parameters, atmospheric composition, and basic parameter settings such as the planet's radius. Together, program and input data form what we call the planetary toolbox.

Details on the input data and the actual performance of the model relative to planetary observations will be the subject of another planned article. ~~-, but to advertise the capability,~~ Figure 1 shows simulations of space-based nadir observations of the 100-300 GHz spectral region for the four different planets. Quite different molecular species dominate this spectral region for the different planets: SO<sub>2</sub> and H<sub>2</sub>SO<sub>4</sub> spectral features on a background of collision-induced CO<sub>2</sub> absorption for Venus, and prominent O<sub>2</sub> and H<sub>2</sub>O lines with some minor O<sub>3</sub> features for Earth. For Mars, one mostly sees the surface, with some very narrow emission lines (H<sub>2</sub>O, CO), due to the very thin atmosphere. For Jupiter, the most prominent feature is a strong PH<sub>3</sub> line, that sits on an absorption background due to NH<sub>3</sub>, modulated by several broad H<sub>2</sub>S absorption features.

There are some caveats for the spectra in Figure 1. First of all, shown are nadir brightness temperatures, which should be kept in mind when comparing to disk integrated measured brightness temperatures. Second, these are clear-sky simulations, neglecting the influence of cloud or precipitation particles, which may affect observed spectra. Third, especially the NH<sub>3</sub> absorption for Jupiter has been shown to be highly sensitive to the choice of spectral line shape (Encrenaz and Moreno, 2002); we have used a Voigt shape. Last, of course, spectra may differ also strongly for other atmospheric scenarios.

Besides the planetary toolbox, there were numerous other additions and improvements: To start with, ARTS now includes collision induced absorption continua from the HIgh-resolution TRANsmission molecular absorption database (HITRAN, Richard et al., 2012). This addition was ~~triggered~~ motivated by the urgent need for some of these continua for other planets, but they may be useful for Earth as well.

Another change is, that the program generally has far fewer internal constants now, which instead are read from input files; or that rather can be read, because there are still built-in default values for convenience. This applies for example to isotopologue ratios and to spectroscopic partition functions. Also in the area of spectroscopy, pressure broadening has been generalised to use separate broadening parameters for all major broadening gas species of the different planets.

Capabilities to simulate active observations have been enhanced by ~~handling simple radar backscattering (without multiple scattering), and by~~ correctly treating Faraday rotation for radio links. The Faraday rotation implementation of this effect uses

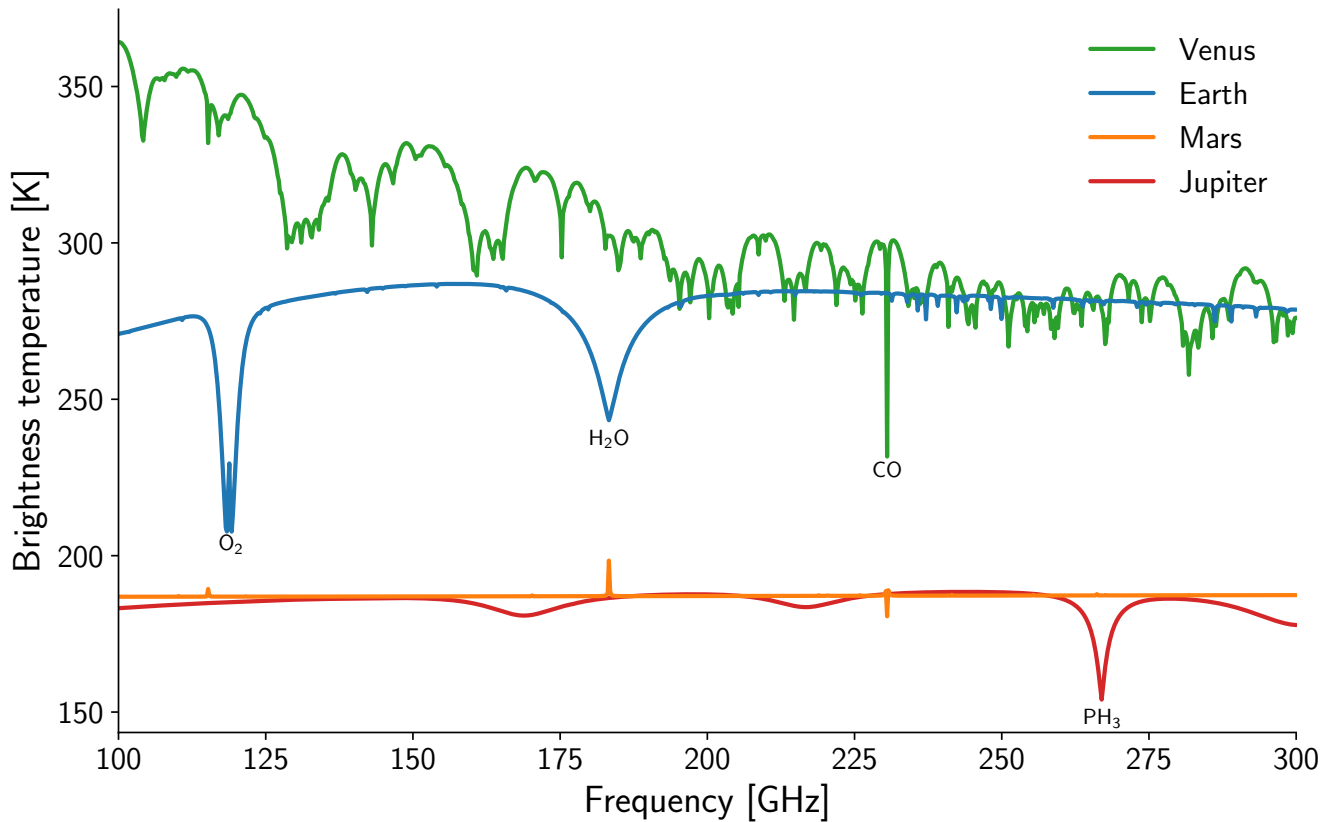


**Figure 1.** Simulated millimeter-wave nadir observations from space for four different planets. The atmospheric scenarios are the same as the ones behind Table 2 (vertical profiles, although the table just lists the data for a single pressure level). Surface reflectivity was assumed to be 0.4 for Earth, 0.13 for Mars, and does not play a role for the other two planets. The large spectral variability for Venus is caused by SO<sub>2</sub>.

a Stokes vector formalism where the extinction term in the scalar radiative transfer equation is replaced by a four-by-four propagation matrix.

~~The Stokes formalism for Faraday rotation~~ [This](#) has benefited greatly from the experience gathered with the last important addition that has to be mentioned here: the capability to simulate [oxygen](#) Zeeman splitting in a physically rigorous way, which is also handled by a Stokes vector formalism, described in Larsson et al. (2014); Larsson (2014). The method has been validated against observations in uplooking (Navas-Guzmán et al., 2015) and downlooking (Larsson et al., 2016) geometry, and also has already been employed for some sensitivity and retrieval simulation studies (Larsson et al., 2013, 2017).

The main purpose of this article is to introduce, explain, and document these recent extensions and modifications, and to serve as a reference for this version of ARTS. The structure is as follows: Section 2 describes the planetary toolbox extensions and modifications, Section 3 describes other modifications and extensions, and Section 4 contains summary and outlook.

## 2 From Earth to planets: generalized propagation modeling methods

When extending radiative transfer modelling from Earth to other planets, the major challenge is to remove a number of assumptions on basic physical parameters made in the model itself or in the input data. ~~This includes hard-coding of~~ Issues include hard-coded constants that are valid (and constant) ~~for Earth~~ for Earth, but might differ between planets. ~~It furthermore regards~~ They furthermore include assumptions in certain algorithms and ~~parametrisations~~ parametrisations. The most prominent one is the expression of spectroscopic parameters of gas absorption lines like foreign pressure broadening and pressure induced frequency shifts by a single parameter valid for the standard mixture of air (79% N<sub>2</sub>+21% O<sub>2</sub>). Here, the limitation is not only in the RT model itself, but ~~spectroscopic catalogues~~ also in the spectroscopic catalogues, which commonly report the Earth-valid ~~standard air parameters only~~.

ARTS has been revised for such assumptions, and modifications towards more general approaches have been made. Below we detail the most relevant of them.

### 2.1 Line spectroscopy

Spectral lines are broadened by collision of gas molecules with other gas molecules. The line width then scales with the partial pressure of the perturbing species. The constant of proportionality is specific to each transition and to the species involved.

Commonly in line-by-line absorption modeling, self broadening and foreign or air broadening are distinguished. The total line width is the sum of the self broadened line width and the foreign broadened line width. The self broadened line width scales with the partial pressure of the species itself, while the foreign broadened line width scales with the total pressure minus the partial pressure of the species itself. (For an explicit mathematical formulation, see Equation 1 further down.) It is typically the respective broadening proportionality constants, or broadening coefficients, of self and foreign broadening, which are reported in the spectral line catalogues.

For line catalogues focusing on Earth applications, the reported foreign broadening coefficient is derived for a standard air mixture of 79% N<sub>2</sub> and 21% O<sub>2</sub>. When considering other planets than Earth, the assumption of air as a nitrogen-oxygen-mixture does not hold anymore. Instead, the composition of the atmosphere ~~largely varies~~ varies hugely from planet to planet. ~~Since pressure,~~ as illustrated by the example atmospheric compositions shown in Table 2.

Pressure broadening is specific to the species involved, and this is also illustrated in Table 2, for the example of the 183 GHz water vapor line. ~~Since~~ atmospheric composition affects the pressure broadening. ~~Hence, for exact calculations,~~ the true composition ~~needs to be considered~~ must be considered for exact calculations. The consequences of not calculating the broadening correctly can be drastic: In a recent comment, Turbet and Tran (2017) point out that using air instead of the correct CO<sub>2</sub> broadening coefficients may lead to an error of 13 K in the surface temperature in climate simulations for early Mars.

In principle, this the impact of the basic atmospheric composition of another planet on the line broadening can be and often is handled in the way that the concept of a foreign broadening coefficient given for a standard air mixture is kept. This requires the compilation of spectral line catalogues specific to the atmospheric composition in question, i.e., the compilation of catalogues specific to individual planets. A more flexible option, though, is to explicitly report broadening parameters for the variety of

**Table 2.** Basic composition of different planets. The table lists VMR values at 700 Pa for some basic model atmospheres that are distributed with ARTS as part of the ‘arts-xml-data’ package. (See documentation in arts-xml-data for data origin, the used scenarios are: Venus: Venus.vira.day; Earth: Fascod/tropical; Mars: Ls0.day.dust-medium.sol-avg; Jupiter: Jupiter.mean.) The last row, ‘ $T$ ’ lists temperature values from the same atmospheres. The last column, ‘ $\gamma$ -183’, lists pressure broadening parameters of the 183-GHz H<sub>2</sub>O line in kHz/Pa. Note that the VMRs are not normalized, so they do not exactly add up to 1 for each planet. Also note that these are only the gases for which we have dedicated broadening parameters; all planets also have other tracegases that are spectroscopically active.

	Venus	Earth	Mars	Jupiter	$\gamma$ -183
N <sub>2</sub>	4.4%	78%	2.7%		31
O <sub>2</sub>	5.1e-7	21%	9.7e-4		20
H <sub>2</sub> O	6.2e-7	4.5e-6	1.5e-4	5.0e-11	155
CO <sub>2</sub>	97%	3.3e-4	95%	3.9e-12	51
H <sub>2</sub>			1.0e-5	86%	24
He				14%	7
$T$	203	241	204	155	

broadening gases in the line catalogue and derive the foreign broadening coefficient from them just-in-time considering the actual atmospheric composition. The latter approach has been chosen for ARTS.

In addition to the line broadening, gas molecule collisions cause pressure dependent frequency shifts of the transitions, also called pressure shifts. Just as the broadening, the pressure shifts are specific to each transition and the species involved in the collision. Commonly, only an overall pressure shift parameter is reported in line catalogues and applied in the line-by-line absorption modeling. Regarding applicability in atmospheres of different compositions, similar considerations as presented for line broadening apply to pressure shifts.

Earlier ARTS versions (Buehler et al., 2005a; Eriksson et al., 2011a) follow the common approach of standard air foreign broadening and pressure shift parameters, calculating the pressure broadened line width  $\gamma_L$  as

$$\gamma_L = x_s p \gamma_s \left( \frac{T_{\text{ref}}}{T} \right)^{n_s} + (1 - x_s) p \gamma_a \left( \frac{T_{\text{ref}}}{T} \right)^{n_a}, \quad (1)$$

where the first term on the right hand side denotes the self broadening width  $\gamma_{L_s}$  and the second one the foreign or air broadening width  $\gamma_{L_a}$ . In Equation 1,  $\gamma_s$  and  $\gamma_a$  are the self and the air broadening parameters,  $n_s$  and  $n_a$  are the temperature exponents for  $\gamma_s$  and  $\gamma_a$ , respectively, and  $T_{\text{ref}}$  is the reference temperature of the broadening parameters. All these parameters are reported in spectroscopic catalogues (the reference temperature often only implicitly for the entire catalogue). Furthermore,  $x_s$  is the volume mixing ratio (VMR) of the transition species,  $p$  is the total atmospheric pressure and  $T$  is the atmospheric temperature.

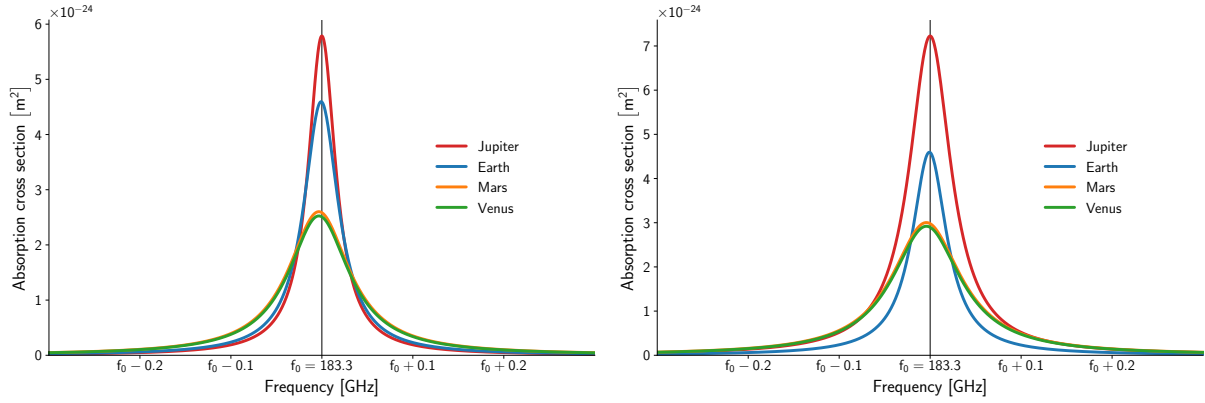


**Figure 2.** Absorption cross section of the 183 GHz water vapor line at 700 Pa, for the different atmospheric compositions listed in Table 2, assuming a Voigt line shape function. Left: using the Earth atmosphere temperature for all four cases, so that differences are only due to the different pressure broadening coefficients. Right: Taking also the temperature from the different planet scenarios, which affects the line strength, corresponding to the integral under the curves.

The pressure shift  $\Delta\nu$  is calculated as

$$\Delta\nu = p \delta\nu \left( \frac{T_{\text{ref}}}{T} \right) \frac{(0.25 + 1.5 * n_{\text{air}}) (0.25 + 1.5 * n_{\text{a}})}{1}, \quad (2)$$

where  $\delta\nu$  is the pressure shift parameter reported in spectroscopic catalogues. Note that to our knowledge there is no generally accepted formulation for the temperature dependence of  $\Delta\nu$  and that Equation 2 simply reports the expression applied in

5 ARTS, without any claim of general validity. The origin of these values for our model is in Pumphrey and Buehler (2000), which in turn refers to Pickett (1980), but that paper, although it does discuss the theory of the pressure shift temperature dependence, does not give any explicit value suggestions for the exponents. Despite its shortcomings, we decided to keep the expression for continuity, and in lack of a better one.

To allow for flexible air compositions, the foreign broadening width  $\gamma_{La}$  has been reformulated into a weighted sum of the

10 broadening contributions from individual broadening species as

$$\gamma_{La} = (1 - x_s) p \frac{\sum_i [x_i \gamma_i \left( \frac{T_{\text{ref}}}{T} \right)^{n_i}]}{\sum_i x_i}, \quad (3)$$

where  $\gamma_i$  is the broadening parameter of the  $i^{\text{th}}$  broadening species,  $n_i$  its temperature coefficient, and  $x_i$  the VMR of the broadening species. Accordingly, To illustrate the impact of this new treatment, Figure 2 shows the absorption cross section of the same water vapor line in the atmosphere of four different planets.

15 Similarly, pressure shift  $\Delta\nu$  is rewritten as-

has been rewritten as

$$\Delta\nu = p \frac{\sum_i \left[ x_i \delta\nu_i \left( \frac{T_{\text{ref}}}{T} \right)^{(0.25+1.5*n_i)} \right]}{\sum_i x_i}, \quad (4)$$

with  $\delta\nu_i$  being the pressure shift due to the  $i^{\text{th}}$  broadening, or rather shifting, species. Note that, like Equation 2, Equation 4 simply states the formula used in ARTS, without claiming general validity. The shift effect can also be seen in Figure 2, if one looks closely the peaks of the cross section curves for Venus and Mars are noticeably different from those of Earth and Mars.

Commonly, the atmospheric composition is not specified in such detail that the sum over the VMR of all considered species adds up to 1. For the classical approach, Equations 1 and 2, this does not matter as the contribution from all foreign gases is taken into account by weighting the foreign contribution with the total foreign air pressure ( $(1 - x_s) p$ ). For the revised approach, Equations 3 and 4, the normalisation by  $\sum_i x_i$  balances out deviations from a VMR sum of 1.

A completely general approach would have to take into account  $\gamma_i$  and  $n_i$  for all possible atmospheric gas species  $i$ . Since contributions of individual species scale with their VMR, it is sufficient to cover the major atmospheric gas species and neglect minor trace gas species. Currently, ARTS 2.2 considers  $\text{N}_2$ ,  $\text{O}_2$ ,  $\text{H}_2\text{O}$ ,  $\text{CO}_2$ ,  $\text{H}_2$ , and  $\text{He}$  as foreign broadening species. This selection covers the most abundant species in the atmospheres of ~~Earth, Venus, Venus, Earth~~, Mars, and Jupiter, the planets the toolbox has been developed for. The approach itself is generally applicable, and the ARTS implementation could easily be modified to cover further foreign species.

~~Note, that this~~ This new broadening mechanism has theoretical advantages even for Earth's atmosphere. To give an example, the broadening of oxygen lines by water vapor is quite different from stronger than their nitrogen broadening, and complete absorption models such as that of Rosenkranz (1993) take into account this effect, which makes oxygen lines broader in a very wet atmosphere. So far, it was not possible to treat this effect with a generic line-by-line calculation based on an external catalog, but with the species-specific broadening parameters in the new ARTS catalogue it happens automatically, if parameters for the broadening by water vapor are available.

However, the practical difference that this makes for Earth is really small. For the example of the 119 GHz oxygen line, the water vapor broadening parameter is roughly 12% larger than the nitrogen broadening parameter (and the oxygen or self-broadening parameter is quite similar to the nitrogen one). Assuming a water vapor VMR of 1% then increases the total width of the line by only about 0.13%. The reason for the small impact is that there is so much more nitrogen and oxygen which dominates the broadening.

To use the new mechanism in practice, broadening and shift parameters for all broadening gases have to be provided by a line catalogue. We have compiled such a catalogue. Details of the compilation are presented in Section 2.2 below.

It should be noted that both the classical and the revised broadening and shift calculation approach are available with ARTS 2.2 and will be kept in future versions. The approach applied in the actual calculation is governed by the format of the spectral line data provided (for further details see Section 2.2) and requires no specific settings by the user. Since data formats for different line transitions are allowed to differ, it is possible to apply both line calculation approaches within one model run. Having both mechanisms available also simplified the testing of the new and more complex treatment, in order to ensure that the results are consistent with the old treatment where they should be.

## 2.2 Line catalogue

ARTS has its own internal representation of spectral line data that maps naturally to a native catalogue format. Two variants of this internal catalogue data exist, corresponding to the two line broadening and shift algorithms introduced above.

Beside other spectroscopic parameters, the catalogue format related to the classical algorithm, called ARTSCAT-3, contains the air broadening and shift parameters  $\gamma_a$ ,  $n_a$ , and  $\delta\nu$  representative for Earth conditions. Besides its internal formats, ARTS can digest other catalogues with different formats, e.g. the HITRAN format. These other databases typically report ~~“classical” Earth-representative-~~ ‘classical’ Earth-representative spectroscopic parameters, hence their data are internally converted to ARTSCAT-3 format. A detailed description of the ARTSCAT-3 format is given in Eriksson et al. (2011b).

The ARTS internal catalogue format corresponding to the revised line broadening and shift algorithm, called ARTSCAT-4, reports broadening and shift parameter for individual foreign species. As already stated above, the currently covered broadening species are the most abundant species in the atmospheres of ~~Earth, Venus, Venus, Earth,~~ Mars, and Jupiter, namely N<sub>2</sub>, O<sub>2</sub>, H<sub>2</sub>O, CO<sub>2</sub>, H<sub>2</sub>, and He. The complete format definition is given in Table 3.

As part of the planetary toolbox, spectroscopic data have been compiled and made available with the arts-xml-data package. This is not the first effort to create a dedicated spectroscopic line list for ARTS: already in 2005, an ESA funded study lead to a dedicated line list for millimeter/sub-millimeter limb sounding instruments (Perrin et al., 2005; Verdes et al., 2005). However, the old line list covered only selected bands, whereas the new line list covers a much broader spectral range.

In line with the scope of the planetary toolbox, to provide tools and data for propagation modeling in the atmospheres of Venus, Mars, and Jupiter as well as Earth in the spectral domain up to 3 THz, the line catalogue has been generated for gaseous absorption species considered of interest in these planets’ atmospheres and for the range of atmospheric conditions of these planets. An overview of the species considered is given in Table 4.

The foreign species specific spectroscopic line parameters have been compiled from literature or extracted from the HITRAN (High-resolution TRANsmission molecular absorption database, Rothman et al., 2009, 2013), GEISA (Gestion et Etude des Informations Spectroscopiques Atmosphériques, Jacquinet-Husson et al., 2011), and JPL (Jet Propulsion Laboratory, Pickett et al., 1998) spectroscopic databases. The sources of the data are given explicitly and in detail for each molecule in ~~Mendrok et al. (2014)~~ Mendrok and Eriksson (2014). Selected examples of the compilation procedure are detailed below. Species of obvious planetological interest but without line absorption signatures in the THz region, like ethane, germane, ethylene, or benzene, have been neglected.

In order to be able to also use the database for Earth applications, species only relevant in the Earth atmosphere, but none of the other planets (see Table 4) have been included as well. Line parameters of these species have been taken from the HITRAN edition current at the time of compilation (Rothman et al., 2013, update 13.06.2013) and converted to ARTSCAT-3 format without any further changes. Note that using ARTS functionality, users themselves can create ARTSCAT spectroscopic files from HITRAN data, e.g. from more recent editions or updates.

~~When compiling the foreign~~ Foreign species specific line parameters ~~, explicit values have been put where available. These have been~~ have been derived by a careful literature investigation searching for experimental or theoretical studies specifically

**Table 3.** ARTSCAT-4 spectroscopic line data format. Column #0 gives the line entry start marker, the following parameters are separated by one or more blanks.

Column	Parameter	Symbol	Unit
0	'@'	-	-
1	molecule & isotopologue tag	-	-
2	center frequency	$\nu_0$	Hz
3	line intensity	$S_0$	Hz m <sup>2</sup>
4	reference temperature	$T_{\text{ref}}$	K
5	lower state energy	$E_l$	J
6	Einstein A-coefficient	$A$	1/s
7	Upper state stat. weight	$g_u$	-
8	Lower state stat. weight	$g_l$	-
9	broadening parameter self	$\gamma_s$	Hz/Pa
10	broadening parameter $\text{N}_2\text{-N}_2$	$\gamma_{\text{N}_2}$	Hz/Pa
11	broadening parameter $\text{O}_2\text{-O}_2$	$\gamma_{\text{O}_2}$	Hz/Pa
12	broadening parameter $\text{H}_2\text{O-H}_2\text{O}$	$\gamma_{\text{H}_2\text{O}}$	Hz/Pa
13	broadening parameter $\text{CO}_2\text{-CO}_2$	$\gamma_{\text{CO}_2}$	Hz/Pa
14	broadening parameter $\text{H}_2\text{-H}_2$	$\gamma_{\text{H}_2}$	Hz/Pa
15	broadening parameter He	$\gamma_{\text{He}}$	Hz/Pa
16	broadening temp. exponent self	$n_s$	-
17	broadening temp. exponent $\text{N}_2\text{-N}_2$	$n_{\text{N}_2}$	-
18	broadening temp. exponent $\text{O}_2\text{-O}_2$	$n_{\text{O}_2}$	-
19	broadening temp. exponent $\text{H}_2\text{O-H}_2\text{O}$	$n_{\text{H}_2\text{O}}$	-
20	broadening temp. exponent $\text{CO}_2\text{-CO}_2$	$n_{\text{CO}_2}$	-
21	broadening temp. exponent $\text{H}_2\text{-H}_2$	$n_{\text{H}_2}$	-
22	broadening temp. exponent He	$n_{\text{He}}$	-
23	frequency pressure shift $\text{N}_2\text{-N}_2$	$\delta\nu_{\text{N}_2}$	Hz/Pa
24	frequency pressure shift $\text{O}_2\text{-O}_2$	$\delta\nu_{\text{O}_2}$	Hz/Pa
25	frequency pressure shift $\text{H}_2\text{O-H}_2\text{O}$	$\delta\nu_{\text{H}_2\text{O}}$	Hz/Pa
26	frequency pressure shift $\text{CO}_2\text{-CO}_2$	$\delta\nu_{\text{CO}_2}$	Hz/Pa
27	frequency pressure shift $\text{H}_2\text{-H}_2$	$\delta\nu_{\text{H}_2}$	Hz/Pa
28	frequency pressure shift He	$\delta\nu_{\text{He}}$	Hz/Pa
29	quantum number information	-	-

devoted to line broadening and shift by He, H<sub>2</sub>, CO<sub>2</sub>, or H<sub>2</sub>. Furthermore, air broadening and shift parameters reported in the HITRAN database are often deduced from individually determined and reported N<sub>2</sub> and O<sub>2</sub> broadening and shift data. In such cases, we applied the original N<sub>2</sub> and O<sub>2</sub> literature data in our catalogue compilation. ~~However, for a given~~ For some

**Table 4.** Overview of the absorption species covered by the ARTS spectroscopic database. For “planet interest” species, ARTSCAT-4 type data with foreign species specific line parameters has been compiled, while data for “Earth-only” species has been taken from HITRAN without modifications and is provided in ARTSCAT-3 format. Empty data files are provided for “no transition” species, which exhibit no absorption lines within the spectral region of interest of the planetary toolbox, but have to be considered as perturbing species. Species with “ARTS 2.0” history are known species in ARTS’ pre-toolbox version. “New” species have been added in ARTS 2.2 with species data taken from HITRAN (default) or other sources like the JPL database (denoted by ‘\*’).

species group	history	species
planet interest	ARTS 2.0	H <sub>2</sub> O, CO <sub>2</sub> , O <sub>3</sub> , CO, CH <sub>4</sub> , O <sub>2</sub> , SO <sub>2</sub> , NH <sub>3</sub> , HF, HCl, OCS, H <sub>2</sub> CO, H <sub>2</sub> O <sub>2</sub> , PH <sub>3</sub> , H <sub>2</sub> S, HO <sub>2</sub> , H <sub>2</sub> SO <sub>4</sub>
	new	SO*, C <sub>3</sub> H <sub>8</sub> *
Earth-only	ARTS 2.0	N <sub>2</sub> O, NO, NO <sub>2</sub> , HNO <sub>3</sub> , OH, HBr, HI, ClO, HOCl, HCN, CH <sub>3</sub> Cl, HCOOH, O, HOBr
	new	CH <sub>3</sub> OH
no THz transition	ARTS 2.0	N <sub>2</sub>
	new	H <sub>2</sub> , He*

combinations of gas species, absorption line and perturbing gas, the broadening and line shift parameters are often absent in the literature, simply because spectroscopic studies dealing with these line parameters were never performed. In this case, the values quoted in our catalogue have been reasonably estimated, where the estimation strategy could differ from one absorption species to the other.

- 5 In particular, for the line broadening parameters, the values have been estimated from those existing in the literature for similar molecules or transitions. For water vapor, for example, numerous experimental and theoretical studies deal with its pressure broadening by CO<sub>2</sub> (Gamache et al., 2011, and references therein). Comparing the air and CO<sub>2</sub> broadening parameters we estimate them being related by  $\gamma_{\text{CO}_2} \sim 1.55\gamma_a$ , and we used this expression in our catalogue compilation to derive  $\gamma_{\text{CO}_2}$  anytime it is otherwise unknown. Similarly, for water vapor transitions we estimated from the existing literature values  $\gamma_{\text{N}_2} \sim$
- 10  $1.1016\gamma_a$ ,  $\gamma_{\text{O}_2} \sim 0.6178\gamma_a$ , and  $\gamma_{\text{He}} \sim 0.24\gamma_a$ . For ozone,  $\gamma_{\text{N}_2} \sim 1.029\gamma_a$  and  $\gamma_{\text{O}_2} \sim 0.89\gamma_a$  were deduced from the literature. We applied these relations to derive the respective  $\gamma_i$  from  $\gamma_a$  quoted in HITRAN for all water and ozone lines for which this information is otherwise missing. For ozone and other molecules, for which no  $\gamma_{\text{He}}$  data exist in the literature, a default relation of  $\gamma_{\text{He}} = 0.25\gamma_a$  was used to estimate  $\gamma_{\text{He}}$ . Regarding  $\gamma_{\text{N}_2}$  and  $\gamma_{\text{O}_2}$ , we carefully checked that their values are consistent with their HITRAN  $\gamma_a$  counterpart, i.e. to fulfill the condition  $\gamma_a = 0.79\gamma_{\text{N}_2} + 0.21\gamma_{\text{O}_2}$  whenever this scaling strategy was applied.
- 15 For several linear molecules, like CO, HCl, HF and CO<sub>2</sub>, a polynomial dependence of the N<sub>2</sub>, O<sub>2</sub> and CO<sub>2</sub> broadening parameters ~~to~~ on the rotational quantum numbers  $m$  was established from measurements reported in the literature (Le Moal and Severin, 1986; Varanasi, 1975). For our compilation, we derived the  $\gamma_{\text{N}_2}$ ,  $\gamma_{\text{O}_2}$ , and  $\gamma_{\text{CO}_2}$  using these expressions.

For some other molecules, e.g. SO<sub>2</sub>, very precise line broadening parameters exist in the literature, however only for a very restricted set of rotational transitions when compared to the full list of lines in the spectral region up to 3 THz. Clearly, it is

not possible to estimate the rotational dependence of these broadening parameters from these limited data. In these cases, the mean values deduced from the experimental data were implemented in our catalogue compilation.

For cases when the pressure broadening parameter of a perturber is not known at all, the default value adopted in HITRAN ( $\gamma_i = 0.1 \text{ cm}^{-1}/\text{atm}$  corresponding to  $\gamma_i = 30000 \text{ Hz}/\text{Pa}$  in terms of SI units as applied in ARTS) was used. Similarly, the default value  $n_i = 0.75$  was set for the pressure broadening temperature exponent. One exception here is helium, for which the default value was estimated as  $\gamma_{\text{He}} = 0.04 \text{ cm}^{-1}/\text{atm}$  (12000 Hz/Pa). The pressure shift parameter  $\delta\nu$ , which is often unknown in the THz region for most of the perturbing gases considered here, has been set to a default value of zero in the absence of any data in the literature.

As indicated above, the primary source for perturber independent parameters like line positions and intensities has been the HITRAN and GEISA databases. However, several molecules considered of interest in planetary atmospheres ~~specifically in the atmospheres of the three terrestrial planets we focused on here~~, are so far not covered by HITRAN or GEISA. This concerns for example sulfur monoxide (SO), sulfuric acid ( $\text{H}_2\text{SO}_4$ ), propane ( $\text{C}_3\text{H}_8$ ) and phosphine ( $\text{PH}_3$ ). To generate the linelists for our catalogue, we used the line positions and intensities quoted in the JPL catalog. The line shape parameters were implemented using the same procedure as described above.

It should be noted that the applied strategy — preferring explicit per-species broadening and shift parameters over deriving them from HITRAN  $\gamma_a$  as well as occasional application of parameterisations in terms of quantum numbers — can lead to differences in Earth atmospheric absorption cross sections when calculated from the toolbox catalogue compared to purely HITRAN-based calculations.

Along with the toolbox development, ARTS' list of known absorption species has been revised. It was updated with data from the recent HITRAN (Rothman et al., 2009, 2013) and TIPS (Total Internal Partition Sums, Fischer et al., 2003; Laraia et al., 2011) editions, which introduced a number of new species and isotopologues. Some further species not (yet) in HITRAN, but required for the planetary toolbox, have been added with species data (molecular mass, isotopologue ratio, partition function information) taken from the JPL spectroscopic database (Pickett et al., 1998, retrieved from <http://spec.jpl.nasa.gov/>) or from educated guesses. The latter regards species that were rated as being of interest in the atmospheres of the toolbox planets and for which spectroscopic line data have been collected (e.g.,  $\text{C}_3\text{H}_8$ ), but also inert species that are required for the planet-suitable line broadening and shift algorithm introduced (e.g., He). Newly added species are identified in Table 4.

The spectroscopic catalogue data are available from the arts-xml-data package, where data are organised into one file per absorption species. It should be noted that our spectroscopic catalogue is a snapshot in time of the available spectroscopic data of interest for planetary atmospheric remote sensing, at the time of development. The snapshot is as of early 2012, when the catalogue was compiled.

HITRAN, the most commonly used general spectroscopic line database has been undergoing very significant development in recent years (Hill et al., 2013). The new 2016 edition for the first time includes explicit broadening parameters for  $\text{H}_2$ , He, and  $\text{CO}_2$  (Gordon et al., 2017), as well as many other new crucial parameters, for example for handling line mixing. We enthusiastically welcome the new HITRAN paradigm, since it means that it will be possible to drive the new broadening

calculation in ARTS with parameters directly from HITRAN in the future. The ARTS interface to the new HITRAN is not yet available, but will be worked on with high priority.

### 2.3 Refractivity

~~Changes in~~ Changes in the propagation speed of electromagnetic radiation ~~, described~~ can lead to a bending of the propagation  
 5 path, called refraction. This is quantified by the refractive index  $n = c/\nu_p$  or the refractivity  $N = n - 1$ , where  $\nu_p$  and  $c$  are  
 the propagation speed in ~~a the~~ the medium and in vacuum, respectively, ~~lead to bending of the propagation path of radiation, also~~  
~~called refraction~~. Neutral gases as well as free electrons contribute to refraction in planetary atmospheres.

Assuming that the refractivity of a gas is proportional to its density (e.g. Newell and Baird, 1965; Stratton, 1968), it can be  
 determined from the refractivity at reference conditions (pressure  $p_{\text{ref}}$  and temperature  $T_{\text{ref}}$ ) and applying a gas law to scale it  
 10 to other conditions. For a gas mixture, the total refractivity can then be determined as the sum of all partial refractivities, i.e.

$$N = N_{\text{ref},1} \frac{n_1}{n_{\text{ref},1}} + N_{\text{ref},2} \frac{n_2}{n_{\text{ref},2}} + \dots \quad (5)$$

where  $N$  is the total refractivity,  $N_{\text{ref},i}$  is the partial refractivity for gas  $i$  at reference conditions,  $n_i$  is the partial density, and  
 $n_{\text{ref},i}$  is the reference density. ~~For Earth-~~

For Earth's atmosphere, commonly empirical parametrizations are applied that summarise the air, or at least its dry part,  
 15 into one component scaled by the total pressure. Water vapor is often considered as a separate component due to its different  
 reference refractivity and its strong variability in abundance (e.g., Thayer, 1974; Mathar, 2007). With  $N_{\text{ref},i}$  being specific  
 to the gas species and varying notably between different species, it is obvious that further refined or generalized models are  
 necessary when atmospheric composition is fundamentally different from Earth.

In ARTS 2.2, we have implemented the approach outlined in Equation 5 with species  $i$  being individual atmospheric gas  
 20 species. The effect of this for the refractivity profile of different planets is shown in Figure 3.

Reference refractivities of  $\text{N}_2$ ,  $\text{O}_2$ ,  $\text{CO}_2$ ,  $\text{H}_2$ , and He, derived at 47.7 GHz and considered to be valid for microwave and  
~~submillimeter-wave~~ submillimeter-wave frequencies, have been taken from Newell and Baird (1965). To achieve a better  
 agreement with parametrisations for Earth,  $\text{H}_2\text{O}$  is considered, too, and its reference refractivity has been estimated from the  
 parametrisation by Thayer (1974). It is  $\text{H}_2\text{O}$  that is causing the kink at high densities (near the surface) for Earth in Figure 3.

25 For scaling to non-reference conditions, we apply the ideal gas law yielding

$$N = \frac{T_{\text{ref}}}{p_{\text{ref}}} \sum_{i=1}^m N_{\text{ref},i} \frac{p_i}{T} \quad (6)$$

where  $p_i$  is the actual partial pressure of species  $i$  and  $T$  the actual temperature. To account for missing contributions of  
 unconsidered species, the refractivity derived from Equation 6 is normalized to a total volume mixing ratio of 1, similar to the  
 line broadening normalisation in absorption calculations (see Section 2.1). ARTS offers further models specifically for Earth  
 30 air refractive indices for the microwave (Thayer, 1974) and the infrared spectral region.

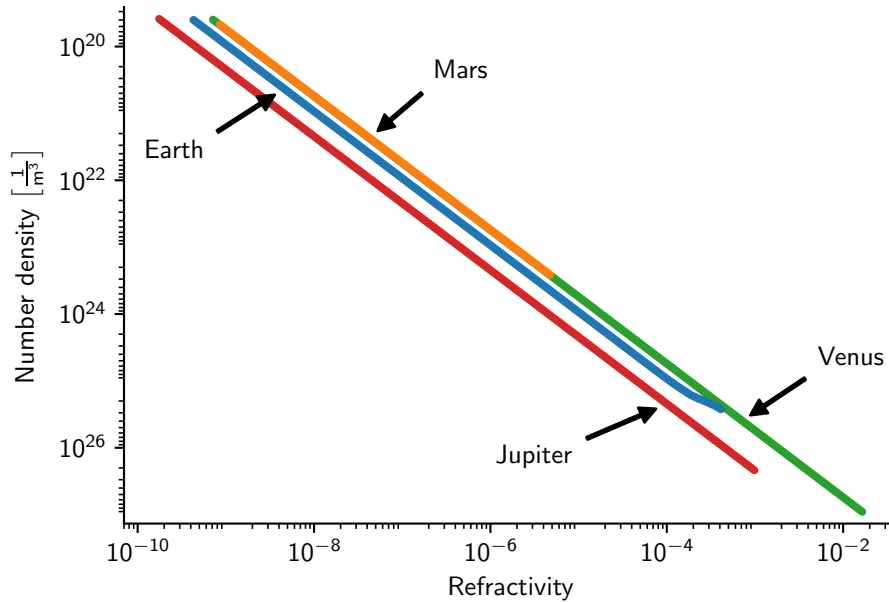


**Figure 3.** Refractivity profiles for different planets. Density is used here for the vertical scale instead of pressure, because otherwise the figure is complicated by the widely different temperatures on different planets leading to different densities at similar pressures. The model atmospheres here are the same as in Figure 1 and described in the caption of Table 2. Data begin at the planets surface, except for Jupiter where they begin at the lowest level of our model atmosphere.

Electron contributions are negligible for passive observation techniques, but play a recognizable role for some active techniques like radio links and Global Navigation Satellite System (GNSS) measurements -(discussed in Section 3.1).

Neglecting influences of any magnetic field, the refractive index of a plasma like the ionosphere is (e.g., Rybicki and Lightman, 1979)

$$5 \quad n = \sqrt{1 - \frac{N_e e^2}{\epsilon_0 m \omega^2}}, \quad (7)$$

where  $\omega$  is the angular frequency ( $\omega = 2\pi\nu$ ),  $N_e$  the electron density,  $e$  and  $m$  the charge and the mass of an electron, respectively, and  $\epsilon_0$  the permittivity of free space. This refractive index, which is less than unity but approaching unity with increasing frequency, describes the phase velocity of the radiation, hence determines the ray path.

The propagation speed of the signal energy through the plasma, which determines signal delays along the path, is described  
10 by the group velocity and the corresponding group refractive index (Rybicki and Lightman, 1979)

$$n_g = \left(1 - \frac{N_e e^2}{\epsilon_0 m \omega^2}\right)^{-1/2} = \frac{1}{n}. \quad (8)$$

~~Electron contribution~~ The electron contributions to the phase and the group velocity index of refraction according to Equations 7 and 8 ~~has have~~ been implemented in ARTS 2.2.

## 2.4 Isotopologue abundances

Absorption coefficients are proportional to the amount of the absorption species and the transition line strength. For practical reasons, the amount is often provided in terms of the volume mixing ratio (VMR) of the species covering all isotopologues, e.g. water vapor VMR instead of the VMR of specific isotopologues like  $\text{H}_2^{16}\text{O}$  or HDO. Then, scaling by the relative abundance of the isotopologue is required. The scaling can either be applied to the VMR or the line strength. HITRAN implements the latter approach by providing pre-scaled line strengths valid for mean Earth conditions. However, as isotopologue abundances differ between planets, this approach is inflexible and inconvenient for planetary applications. ARTS on the other hand applies the VMR scaling approach requiring isotopologue abundance independent line strengths.

For being able to apply HITRAN spectroscopic data, ARTS contains a hard-coded table of relative isotopologue abundances in the Earth atmosphere, where the relative abundance is the ratio of abundance of an isotopologue to the abundance of the gas species over all its isotopologues (in contrast, isotopologue ~~ratio-ratio~~ refers to the abundance ratio of an isotopologue to the abundance of the main isotopologue of the species; ~~equivalent definitions apply for isotopes~~). This table is used to convert HITRAN isotopologue scaled line strengths into ARTS' abundance independent line strengths. In previous ARTS versions, the table was also applied in the VMR scaling of absorption coefficients. In ARTS 2.2, isotopologue abundance has been introduced as a user-accessible variable, which can be initialized from the built-in isotopologue table, e.g. for Earth atmosphere calculations, or read from file, e.g. for planetary use.

As part of the planetary toolbox, tables of relative isotopologue abundances for Venus, Mars, and Jupiter are provided with the arts-xml-data package. ~~Typically, isotopic composition of atmospheres is reported, commonly in terms of isotope ratios, from which isotopologue abundances of molecular species can be derived. The tables provided here have been derived~~ We generated these, based on the available planetary literature. What can readily be found there are not isotopologue abundances for all different molecules, but rather isotope ratios for important atoms, for example the ratio of deuterium to normal hydrogen. From these, we generated the molecular isotopologue tables by rescaling Earth isotopologue abundances with the planetary isotope ratios ~~retrieved from literature, reported in Table 5.~~

Isotope ratios of D (in all planets) and  $^{15}\text{N}$  (in Mars and Jupiter) were found to significantly differ from Earth values, while other species are within 5% of ~~Earth's~~ their Earth values. Adaptation of isotopologue abundances was, hence, restricted to species containing hydrogen and nitrogen. ~~Isotopic ratios applied in the adaptation are reported in Table 5. Earth values were derived from ARTS built-in isotopologue abundances separately per molecular species, hence only an approximate value is given in the table.~~

~~Planetary isotopic ratios as applied in the isotopologue ratio conversion. Earth values are given for reference only, while species specific values were applied in the conversion (see text). Values for Venus, Earth and Mars taken from Lammer et al. (2008, Table 1), Jupiter from Owen and Encrenaz (2003). Planet D/H  $^{15}\text{N}/^{14}\text{N}$  Venus  $1.9\text{e-}2$  as Earth Earth ( $\sim 1.5\text{e-}4$ ) ( $\sim 3.7\text{e-}3$ ) Mars  $8.1\text{e-}4$   $5.7\text{e-}3$  Jupiter  $2.6\text{e-}5$   $2.25\text{e-}3$  For spectral lines belonging to molecules that contain heavy hydrogen or nitrogen atoms, the~~

**Table 5.** Planetary isotopic ratios as applied in the isotopologue abundance data table generation. Values for Venus, Earth and Mars taken from Lammer et al. (2008, Table 1), Jupiter from Owen and Encrenaz (2003). The Earth values are given for reference only, because in the actual table generation we inferred them from the HITRAN Earth Isotopologue abundance for each individual molecule.

Planet	D/H	$^{15}\text{N}/^{14}\text{N}$
Venus	1.9e-2	as Earth
Earth	(1.5e-4)	(3.7e-3)
Mars	8.1e-4	5.7e-3
Jupiter	2.6e-5	2.25e-3

change in absorption due to these abundance differences can be very significant. To give an example, the isotopologue abundance of HDO is more than 100 times that of Earth on Venus, 5 times that of Earth on Mars, and only less than 0.2 that of Earth on Jupiter. Because absorption is proportional to abundance, these differences translate directly into absorption differences for spectral lines belonging to this species.

## 5 2.5 Further adaptations for planetary use

~~A couple of further~~ Several other planet dependent parameters have also been turned into user-controllable parameters. This includes size and shape parameters of ellipsoidal planets, required for line of sight calculations, where also predefined settings for the toolbox planets in the form of dedicated workspace methods are available. This furthermore concerns settings of the gravitational constant and of the molar mass of dry air, both required for deriving altitude-pressure relations assuming hydrostatic equilibrium, as well as the sidereal rotation period of a planet, required for considering Doppler shifts resulting from the rotation of a planet observed from a platform not in orbit around this planet (see Section 3.2.4).

## 3 Further new model features and remaining restrictions

Besides the adaptations described above, which were necessary to make the propagation model applicable to general planetary atmospheres, several other new modeling features are available with the new ARTS version. ~~A major extension is the coverage of additional measurement techniques, specifically of active techniques like~~ An example is the addition of radio occultation measurements and radio link budget estimations (Section 3.1), ~~but also backscattering radar observations (Section ??). The first ones are which is~~ of particular interest for the planetary toolbox since ~~they have been suggested or applied~~ such measurements are relevant for planetary exploration (e.g. Eshleman et al., 1987; Hinson et al., 1997; Oschlisniok et al., 2012). ~~Several~~ Some physical processes affect both passive and active measurements. ~~Propagation models applying~~ The fact that ARTS uses identical algorithms to model these processes ~~provide~~ provides consistent simulations of both techniques. ~~Below, we describe each of the newly available measurement technique capabilities in detail.~~

~~New ARTS features also cover a number of physical processes affecting electromagnetic propagation, which were neglected before~~ In this release, some physical processes that were not treated before have been added. These include for example Doppler

shifts due to wind and planet rotation, the [oxygen](#) Zeeman effect, Faraday rotation, and dispersion, which all are described in Section 3.2. In order to model several of these effects, additional model input characterising the atmosphere is required. Section 3.3 provides details on the handling of these input parameters.

Active measurement techniques provide more diverse measurement parameters. Therefore, the measurement module output has been extended. This also allows for more detailed output for passive measurement simulations. An overview is given in Section 3.4.

### 3.1 Radio link budgets

A basic handling of radio link budgets has been introduced. The implementation focuses on [the](#) attenuation of the power between a transmitter of a coherent signal and the receiver position, but also some other aspects are covered by the auxiliary variables provided. The latter includes a basic treatment of radio occultation, i.e. when a coherent microwave signal, such as from GNSS, is recorded by either a satellite- or ground-based receiver in order to determine certain atmospheric properties (e.g. Kursinski et al., 2000; Nilsson and Elgered, 2008). Only an overview of these additions is given here, for details see Eriksson et al. (2011c) and the built-in documentation.

The most critical step of these calculations is to establish the propagation path between transmitter and receiver. This step is so far only handled by a quite simple and time consuming algorithm (Eriksson et al., 2011c) and only considers effects covered by geometrical optics. ~~So~~ [Snell's law is used to determine the bending of the radiation as it travels through the atmosphere, and the algorithm looks for a path that connects transmitter and receiver. In reality, there can be more than one possible path for atmospheres with strong vertical temperature gradients \(so called multi-pathing](#) ~~is not treated, the algorithm settles with finding a single-~~), but this is currently not treated in ARTS. [The algorithm simply finds a link path, or to determine determines](#) that no path is possible, due to interception by the planet's surface.

~~On the other hand, the~~ [The](#) receiver and transmitter can be placed at arbitrary positions, allowing that, for example, satellite-to-satellite as well as aircraft-to-ground radio links can be analysed. All atmospheric dimensionalities are handled (1D, 2D and 3D).

~~The dominating attenuation term is the~~ [“Attenuation due to gases and particles are included exactly in the same manner as for pure transmission calculations, but an important additional attenuation term, that is in fact dominating, is the ‘free space loss’”](#). This term is in ARTS defined as  $1/(4\pi l^2)$ , where  $l$  is the distance along the line of sight. A probably more common definition of the term, [based on the ‘Friis transmission formula’](#), is  $(\lambda/(4\pi l))^2$ , where  $\lambda$  is the wavelength ~~,-but this version is avoided as it includes-~~ (see e.g. Ulaby et al., 2014, Sec. 3.3). [We avoid the later version because the additional  \$\lambda/\(4\pi\)\$  forefactor is meant to account for](#) the variation of the receiver's gain with frequency, while in ARTS the ambition is to keep atmospheric and sensor effects strictly apart. ~~Attenuation due to gases and particles are included exactly in the same manner as for pure transmission calculations.-~~

A special effect when transmitting coherent signals is (de)focusing. Simply expressed, the effect originates in the fact that refraction can vary over the wavefront. Defocusing occurs if neighbouring ray-paths in a medium diverge more quickly than for free space propagation. The opposite, focusing, can also take place, but is in general less pronounced. ARTS provides a general

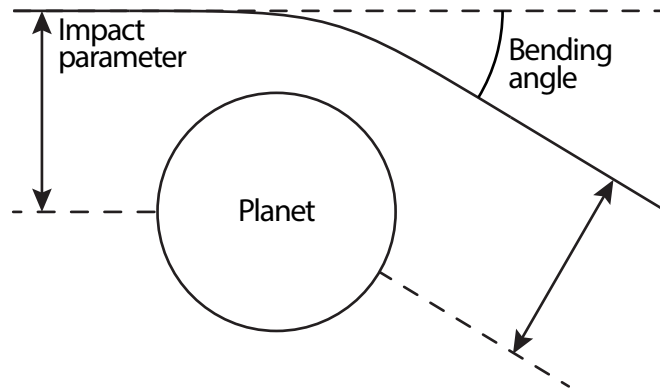


**Figure 4.** The radio occultation geometry with impact parameter and bending angle. See for example Kursinski et al. (2000) for details.

and rough estimate of (de)focusing by simply determining the propagation path at two slightly shifted propagation angles, starting at the transmitter, and comparing the distance between the two paths, at the receiver, to the distance expected from pure geometry. For satellite-to-satellite links, the user can instead select to make use of some standard analytical approximations (e.g. given in Kursinski et al., 2000, Sec. 3.7), where both the defocusing and focusing components are considered.

- 5 For a more complete characterisation of the radio link, the auxiliary output at hand includes the following quantities: bending angle, impact parameter (both defined as in Figure 4), extra path delay, Faraday rotation ([see Section 3.2.2](#)) and all loss terms reported individually.

### 3.2 Back-scattering radars

~~Another active technique now partly treated is atmospheric back-scattering radar. The module for this task, developed as part of Galligani et al. (2015), handles the direct back-scattering together with atmospheric propagation and attenuation, giving full consideration of polarimetric aspects in both parts. Features not yet treated include the influence of the planet's surface, multiple scattering and Doppler shifts of the radar pulse itself. Multiple scattering refers here to the reception of photons scattered more than once, while two-way attenuation due to particle absorption and scattering is considered. That is, when multiple scattering is significant, the simulated radar return will be an underestimation of the true value; see Battaglia et al. (2010) for a review when multiple scattering requires consideration. An application example of this is shown in Figure 5, which makes use of operational atmospheric analysis data from the European Centre for Medium-Range Weather Forecasts (ECMWF), as well as a co-located radio-occultation observation from the GNSS Receiver for Atmospheric Sounding (GRAS). In the left panel, it shows the ARTS-simulated bending angle, based on the ECMWF model data, together with observed bending angles for two different GRAS data retrieval algorithms (so-called geometric optics (GO) and full spectrum inversion (FSI)).~~

20 ~~Each observation of back-scattering,  $y$ , is simulated as-~~

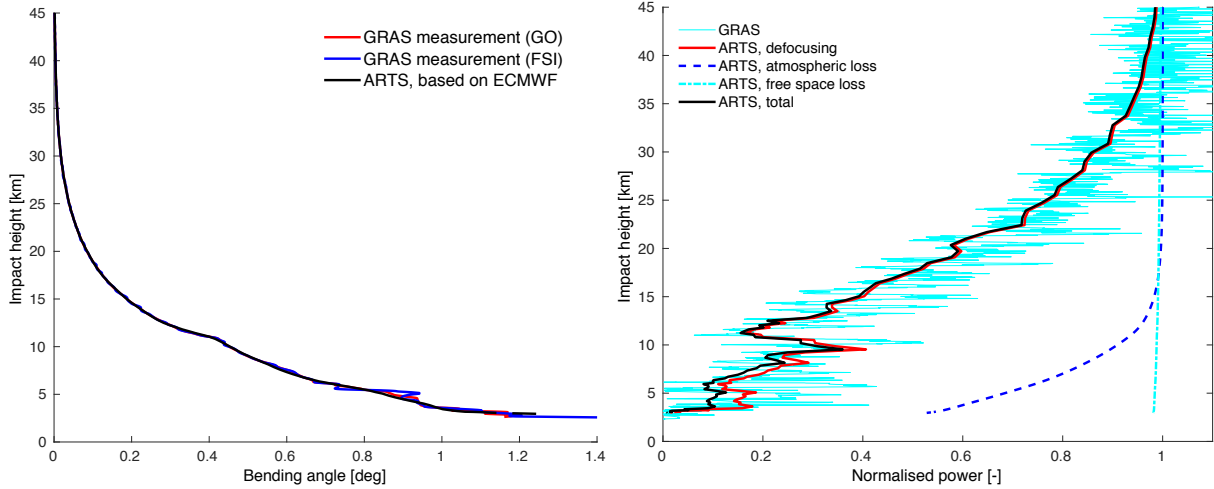


**Figure 5.** Comparison of ARTS forward model calculations with GRAS data. The input to ARTS is ECMWF operational analysis data. The left panel compares ARTS simulations to observed bending angles determined in two different ways from raw GRAS observations. The right panel shows the observed and simulated link budget for transmitted power. As common for radio-occultation observations, the vertical scale, impact height, is simply the impact parameter of Figure 4 minus the Earth radius.

$$\underline{y} = \underline{p} \cdot \underline{T}_h \underline{Z}(\Omega = 180^\circ) \underline{T}_a \underline{s}_t,$$

where  $\underline{s}_t$  is a unit vector representing the transmitted pulse (including its polarisation state),  $\underline{T}_a$  is the transmission from the transmitter/receiver to the scattering point,  $\underline{Z}(\Omega = 180^\circ)$  is In the right panel, Figure 5 shows the observed transmitted power from the GRAS instrument, as well as the ECMWF-model-based ARTS simulation, broken down by individual effect. Free space loss is the dominating attenuation mechanism, but varies little during a GRAS occultation. The ‘power’ in Figure 5 is normalised to the free space loss at a high altitude. Atmospheric attenuation (absorption of gases, no scattering included in these calculations) is low in the stratosphere, but is an important factor for low impact heights. However, the value of the scattering (or phase) matrix for backward scattering,  $\underline{T}_h$  is equivalent to  $\underline{T}_a$  but is valid for the opposite direction, and  $\underline{p}$  is vector describing the polarisation response of the receiver. For vector radiative transfer, the transmission can depend on direction, and  $\underline{T}_h$  and  $\underline{T}_a$  are not necessarily equal. The above is an extension of the traditional, scalar, radar equation (e.g. Battaglia et al., 2010, Eq. 1):

$$\underline{\beta}_a(l) = \beta(l) e^{-2\tau(l)},$$

where  $\beta$  and  $\beta_a$  are local and “apparent” back-scattering coefficient respectively,  $l$  is the distance to the radar, and  $\tau$  is the optical depth main variation of power during the occultation is determined by defocusing. The actual GRAS measurement is also affected by scintillations (explaining the most rapid variations of the power), but this mechanism is not treated by ARTS.

The output of Equation ?? can be provided both as a function of altitude or round-trip time, in units of either back-scattering coefficient ( $1/(m\text{-sr})$ ) or radar reflectivity ( $Z_e$ ) (in both cases, the mean inside each altitude or time bin). Observations outside the zenith and nadir directions are allowed.

## 3.2 General radiative transfer features

- 5 This section presents new features in ARTS that are of radiative transfer character and of general applicability, i.e. that can be used together with the different measurement technique modules.

### 3.2.1 Handling of non-particle polarisation

Older ARTS versions have assumed that only particulate matter (including the planet's surface) causes effects that go beyond a scalar description. That is, gaseous absorption has been seen as scalar attenuation coefficients. This limitation is now removed, 10 for two reasons. First of all, the Zeeman effect (Section 3.2.3) causes the absorption to depend on polarisation, which cannot be described in a scalar manner. Secondly, effects of magneto-optical (del Toro Iniesta, 2003, Sec. 1) character also do not fit into a scalar formalism, and both Faraday rotation and parts of the Zeeman effects fall into this category.

Accordingly, the code has been revised to throughout allow for a matrix description of propagation effects. As a consequence, the terminology used in ARTS has also changed, what was before denoted as ~~“absorption coefficient”~~ ‘absorption coefficient’ 15 is now called ~~“propagation matrix”~~ ‘propagation matrix’ (following e.g. del Toro Iniesta, 2003) to reflect the wider scope of the associated variables and methods. This extension made it also possible to add a feature treating particulate matter as purely absorbing matter. This allows for a much faster treatment of radiative transfer when scattering is neglected. This simplification is only valid when the particles are small compared to the wavelength, i.e. their single scattering albedo is small. There is no check in ARTS, though, that this condition is fulfilled; this judgement is fully left to the user.

### 20 3.2.2 Faraday rotation

A wave propagating through the ionosphere will force free electrons to move in curved paths. For example, if the incident wave is circularly polarised, the motion of the electrons will be circular. ~~Consequently~~ As a consequence, the refractive index is not a single constant, but depends on polarisation. ~~More precisely, left and right hand polarised waves will propagate with different speeds. As a plane polarised wave can be thought of as a linear superposition of a left hand and a right hand polarised wave with equal amplitudes but different phase, the plane of polarisation will then rotate as the wave is~~ A manifestation of this 25 ‘Faraday effect’ is that the electric field vector of a wave propagating through the ~~media~~ ionosphere will rotate. This is denoted as Faraday rotation, and this physical mechanism is now handled by ARTS. The core expression is (e.g. Rybicki and Lightman, 1979)

$$r = \frac{e^3}{8\pi^2 c \epsilon_0 m^2 f^2} n_e(s) \mathbf{B}(s) \cdot \hat{\mathbf{s}}, \quad (9)$$

where  $r$  is the change in rotation angle [rad/m],  $e$  is the charge of an electron,  $c$  is the vacuum speed of light,  $\epsilon_0$  is the permittivity of vacuum,  $m$  is the electron mass,  $f$  is the frequency,  $n_e(s)$  is the density of electrons at point  $s$ ,  $\mathbf{B}$  is the magnetic field,  $\cdot$  denotes the dot (scalar) product and  $\hat{s}$  is the unit vector along the propagation direction. That is, the rate of rotation depends on the number of free electrons and the angle between propagation and magnetic field directions. It is also proportional to  $f^{-2}$ , causing Faraday rotation to be negligible above about 3 GHz (Ulaby et al., 2014). See Eriksson et al. (2011c) for further details.

### 3.2.3 Zeeman effect

Molecules with unpaired electrons experience an effect named the Zeeman effect after its discoverer (Zeeman, 1897). The Zeeman effect polarises the radiation as a function of magnetic field orientation, and splits what is otherwise a single spectral line into several lines, with a splitting distance that is a function of the magnetic field strength. The total line strength is kept constant but distributed over the split lines. From an ARTS user perspective, the main practical requirement for Zeeman calculations is that the magnetic field must be specified as an additional input field. Some additional spectroscopic parameters are also needed.

The physical mechanism, from which the effect arises, is that the spin of the unpaired electrons couples to the external magnetic field, changing the energy state of the molecule as a function of magnetic field strength by

$$\Delta E = -gM|\mathbf{B}|\mu_b, \quad (10)$$

where  $g$  is the state-dependent Landé factor,  $M$  is the projection of the total angular momentum number  $J$  along the magnetic field,  $|\mathbf{B}|$  is the magnetic field magnitude, and  $\mu_b$  is the Bohr magneton. See e.g. Figures 4 and 7 in Larsson et al. (2014) for an example of how the Zeeman effect influences the brightness temperature signal as perceived by a sensor.  $M$  belongs to the set  $\{-J, -J+1, \dots, J-1, J\}$ , and can only change by  $-1$ ,  $0$ , or  $1$  during a transition. This makes for a total of  $3(2J+1)$  lines in place of the single original line.

The change in projection of  $J$  is related to the polarisation of the radiation and is influenced by the angle between the magnetic field and the path of propagation of the radiation. If the magnetic field is in the plane of observation, transitions with a changing  $M$  affect linear polarisation along the magnetic field and transitions with a constant  $M$  affect linear polarisation perpendicular to the magnetic field. If the magnetic field is pointing directly towards or away from the observer, only transitions with a changing  $M$  affect the radiation. This radiation will have its circular polarisation state altered. The implementation and the physics of the Zeeman effect in ARTS are described in detail by Larsson et al. (2014) and Larsson (2014), and references therein.

~~From an ARTS user perspective, the main practical requirement for Zeeman calculations is that the magnetic field must be specified as an additional input field. Some additional spectroscopic parameters are also needed. For~~ For this ARTS version, the only tested Zeeman absorption species is molecular oxygen ( $\text{O}_2$ ), ~~the only tested Zeeman absorption species so far, these parameters are included with the ARTS distribution.~~ Other species, like NO and SO, are also Zeeman-affected (see, e.g. Veseth,

1977; Christensen and Veseth, 1978), and while ARTS should be able to model the effect also for these species, this **remains mostly untested at the time of writing** is left to future versions.

The ARTS oxygen Zeeman calculations have been validated in some studies so far: Navas-Guzmán et al. (2015) simulated ground-based observations of mesospheric molecular oxygen spectra in linear polarization for several observational directions, and found good agreement with observations; Larsson et al. (2016) compared the ARTS simulations for a down-looking meteorological sensor to observations and to another, stronger parameterised Zeeman model. The module has also been applied to theoretical studies on mapping Martian surface magnetism (Larsson et al., 2013, 2017).

### 3.2.4 Doppler shifts

A basic treatment of Doppler shifts due to winds has existed in ARTS for some time. For ARTS 2.2 this part was completely recorded, and the Jacobian of observations with respect to the three standard wind components (u, v and w) can now also be calculated. The immediate motivation for this extension was the wind retrievals presented in Rüfenacht et al. (2014). The Doppler shift  $\Delta\nu$  is given as

$$\Delta\nu = \frac{-v\nu_0 \cos(\gamma)}{c}, \quad (11)$$

where  $v$  is the wind speed,  $\nu_0$  is the rest frequency and  $\gamma$  is the angle between the wind direction and the line-of-sight. More details are found in Eriksson et al. (2011c). Note that the Doppler shift caused by the random thermal motion of air molecules is part of the line shape, the function describing the frequency dependence of the absorption of each transition, and is therefore not modeled explicitly here.

The rotation of the planet is another possible cause of Doppler shifts. This effect can be a concern for satellite measurements, but there is no net impact if the observer follows the planet's rotation, such as for ground-based observations of the planet's own atmosphere. In ARTS, this Doppler effect can be included by mapping the planet's rotation to a zonal wind speed, the u component. This pseudo-wind,  $v'_u$ , is calculated as

$$v'_u = \frac{2\pi \cos(\alpha)(r+z)}{t_p}, \quad (12)$$

where  $\alpha$  is the latitude,  $r$  is the local planet radius,  $z$  is the altitude and  $t_p$  is the planet's rotational period. This term is added to the true zonal wind speed.

Further, for moving observation platforms, such as aircraft or satellites, the sensor velocity can result in a significant Doppler shift and ARTS provides now a rudimentary handling of this aspect. However, the platforms are normally moving with a constant speed and the associated Doppler shift is probably most easily handled outside of the forward model.

### 3.2.5 Dispersion

By default, ARTS assumes that the propagation path is common for all frequencies, ~~i.e. that~~ there is no dispersion. ~~This is an approximation, because the~~ In most cases this is a good approximation. The atmosphere is dispersive at frequencies around strong transitions. ~~However, but~~ as discussed in Buehler et al. (2005a), this effect can ~~safely be neglected in practice be~~  
5 ~~neglected,~~ because it is associated with very high absorption. ~~On the other hand~~

~~However,~~ the introduction of ~~Faraday rotation ionospheric refraction (Equation 7),~~ which is frequency dependent (~~see Equation 9),~~ now demanded to add a feature to handle dispersion. This was solved by making it possible to optionally have frequency as the outermost loop in the calculation, so that propagation paths are recalculated for each individual frequency.

This solution is completely general, so that ~~Faraday rotation ionospheric dispersion~~ can be combined with all other features  
10 of ARTS. It also means that dispersion can now be modeled explicitly even if ionospheric refraction is not included, if one is willing to pay the price of significantly increased computational cost for the calculation of the individual ~~frequency-dependant~~ frequency-dependent propagation paths.

### 3.2.6 The $n^2$ radiance law

ARTS has been corrected regarding passive observations, where the  $n^2$  radiance law was not fully considered before. This law  
15 says that, even in the absence of attenuation, the radiance ~~changes would change~~ along the propagation path due to refraction effects. The preserved quantity is (Mobley, 1994; Mätzler and Melsheimer, 2006) ÷

$$\frac{I'}{n^2} \quad (13)$$

where  $I'$  is the uncorrected radiance and  $n$  is the ~~(real part of the) refractive index.~~ refractive index as defined in Section 2.3.

It can be shown that it suffices to consider the refractive index at the point of emission and the point where the measurement  
20 is performed (Mobley, 1994, Eq. 4.23). To incorporate the  $n^2$ -law in the description of emission turns out to be equivalent to replacing the local propagation speed with the ~~vacuum speed in~~ speed of light in vacuum in the Planck blackbody expression. This feature was already in place, but now also a scaling with  $n^{-2}$  at the measurement position is applied in ARTS. This change affects only observations performed within the model atmosphere, as the relevant  $n$  for satellite-based observations is unity. This particular treatment of the  $n^2$ -law is discussed further in Eriksson et al. (2011b).

### 25 3.2.7 Continuum models

A number of gas absorption continuum models are available with ARTS. This particularly covers models for the micro- and millimeter-wave region (e.g. Liebe et al., 1993; Rosenkranz, 1993, 1998), but also several editions of the Clough-Kneizys-Davies continuum model (CKD, Clough et al., 1989, 2005), later enhanced by Mlawer and Tobin (MT\_CKD, Mlawer et al., 2012), models that cover the entire millimeter to infrared spectral range. However, all of these continua have been devel-

oped with focus on Earth observations. In atmospheres with different major atmospheric constituents as well as pressure and temperature conditions, different continua play important roles.

Recent editions of the HITRAN database offer collision-induced absorption (CIA) data (Richard et al., 2012). CIA is caused by collisions of centro-symmetric molecules that possess no permanent electric dipole, like O<sub>2</sub>, N<sub>2</sub>, H<sub>2</sub>, CO<sub>2</sub>, and CH<sub>4</sub>, but for which collisions create a transient dipole. The absorption strength of CIA is characterised by its dependence on the molecular density of both molecular species involved in the collision:

$$\alpha_{i,j} = \kappa_{i,j} n_i n_j, \quad (14)$$

where  $i$  and  $j$  denote the two species involved,  $\alpha$  is the absorption coefficient,  $\kappa$  the binary absorption cross section, and  $n$  the number density of the respective species.

10 Tabulated frequency and temperature dependent  $\kappa_{i,j}$  for a ~~varity~~variety of species  $i$  and  $j$  are available from recent HITRAN editions. For the planetary toolbox with a focus on Venus, Mars and Jupiter, CIA data for CO<sub>2</sub>-CO<sub>2</sub>, H<sub>2</sub>-H<sub>2</sub>, and H<sub>2</sub>-He are of particular interest. A mechanism to consider bi-species dependent absorption has been implemented, where tabulated binary cross sections have to be provided to ARTS. A method to derive  $\kappa_{i,j}$  from HITRAN data is available. To make the HITRAN data ~~seemlessly~~seamlessly work with ARTS, we created a slightly modified version of the data in native ARTS format: data  
15 sets covering the same frequency range have been merged into one frequency-temperature table, data sets only covering visible and shorter wavelengths have been removed, and all binary cross sections have been converted from HITRAN (cm<sup>5</sup>/molec<sup>2</sup>) to ARTS (m<sup>5</sup>/molec<sup>2</sup>) units. These data are available as part of the arts-xml-data package.

### 3.3 Extended atmospheric state characterisation

Several of the new physical processes described above require additional input parameters in order to be properly modeled.

20 Doppler shifts from wind require characterisation of the wind, Zeeman effect and Faraday rotation require magnetic field knowledge, and Faraday rotation and ionospheric refraction require a description of the electron density.

All non-scattering atmospheric matter in ARTS is subsumed as absorption species with associated atmospheric fields gathered into a variable named `vmr_field`. Following this approach, free electrons have been added to the list of allowed absorption species, and when considering free electrons in a radiative transfer calculation, the electron density field (m<sup>-3</sup>) is held as one  
25 entry in `vmr_field`.

Winds as well as the magnetic field are vector parameters, hence require three pieces of information per atmospheric grid point. For both parameters, variables have been created to hold the (up to) three dimensional fields of the individual vector components `u`, `v`, and `w`. Generally, parameters that are not explicitly set are interpreted as equivalent to zero winds and magnetic field components, respectively.

### 3.4 Auxiliary output

The main output of ARTS' radiative transfer part is a vector with all simulated observations appended, i.e. directly matching the ~~“measurement vector”~~ ‘measurement vector’  $y$  in the formalism of Rodgers (2000). Auxiliary data that is input or output of ARTS workspace methods, such as the observational position(s) associated to a radiative transfer calculation, are always at hand. However, in many cases there exists also an interest in additional information calculated inside the radiative transfer methods. A typical example is the optical thickness related to an observational setup. Other commonly requested quantities include absorption, temperature and volume mixing ratios along the propagation path.

A general approach for obtaining such additional auxiliary data has been added to ARTS. The exact set of auxiliary variables that can be obtained differs depending on what radiative transfer problem has been solved. For example, there is no need to cover optical thickness by methods that have atmospheric transmission as main output. The auxiliary variables at hand can be divided into two main classes. The first class is the variables defined along the propagation path (such as temperature and partial transmissions). This class can just be obtained for single pencil beam calculations. This is because there is no common propagation path in the general case, considering a finite field of view, where a weighting of results from different propagation paths with the antenna pattern is performed. The second class consists of quantities resulting in a scalar value for each simulated observation value, that can be provided also for simulations including weighting with sensor characteristics. This class includes optical thickness and flags reporting intersection with the ground or the ~~“cloud box”~~ ‘cloud box’.

### 3.5 Remaining restrictions and outlook

Although ARTS is a fairly general radiative transfer model, several important restrictions remain. Perhaps the biggest one is that there is no collimated beam radiation source, so the model is not suitable for modelling the scattering of solar radiation in the atmosphere. Version 2.2, the subject of this article, also does not allow handling absorption and emission for conditions outside of local thermodynamic equilibrium (non-LTE). This may change in a future release, because work in this direction is ongoing.

Line mixing, a phenomenon where closely spaced molecular energy levels affect the shape of the spectral lines, is also not treated in this version. The phenomenon is important, because it affects two molecules of high scientific interest, CO<sub>2</sub> and O<sub>2</sub>. For the former, line mixing is important for calculating correct energy fluxes, as needed by atmospheric circulation models and ~~simpler~~ radiative-convective equilibrium models. For the latter, line mixing is important for temperature remote sensing in the microwave spectral range. This aspect is in active development, and future releases of ARTS are planned to include line mixing for both species.

Other less prominent restrictions are that ARTS does not handle birefringence, handles ionospheric propagation only at frequencies well above the plasma frequency, and does propagation path calculations only by geometric optics (it is not a wave optics propagator). Also, while the model has simple surface models (specular and Lambertian) or accepts general bidirectional surface reflectivity as input, there is no explicit subsurface model, which might be of interest for complex surfaces such as snow.

## 4 Summary and conclusions

This article ~~described~~describes version 2.2 of the atmospheric radiative transfer simulator ARTS. Its most significant innovation is the planetary toolbox, which allows radiative transfer simulations for other solar system planets, in addition to Earth, but should also benefit the studies of bodies beyond the solar system like exoplanets. The necessary adaptations have made  
5 the program more general in several important aspects, ~~as described above~~, which benefits also applications for Earth's atmosphere. ~~As an example, several parameters that were hardcoded before, such as isotopologue ratios, can now be read from data files, which allows easy sensitivity studies with modified parameter values~~

Besides this extension, there were numerous improvements and developments compared to the last version that is described in the literature (Eriksson et al., 2011a), and the most important of these are also described.

10 We hope that others may find the model useful, and always appreciate comments, suggestions, and usage examples. The best way to get in touch with the model developers is via the ARTS website, given below.

*Code and data availability.* The model, together with extensive documentation, associated tools, and input data, is freely available under a GNU public license from [www.radiativetransfer.org](http://www.radiativetransfer.org). The web page also hosts dedicated email lists for ARTS users and developers. This article is about ARTS version 2.2, the exact subversion number at the time of writing is 2.2.64. There may be a limited number of bugfix  
15 releases that increment the last digit number, but the active development of new features is happening in version 2.3.

*Competing interests.* The authors declare that they have no competing interests.

*Acknowledgements.* We would like to acknowledge the tremendous support from the ARTS developer and user community. For example, they contribute by answering questions by new users on the ARTS email lists.

We also acknowledge financial support, most importantly from the European Space Agency (ESA) in the context of contract No 4000104175/11/NL/AF  
20 ~~“Microwave propagation toolbox for planetary atmospheres”~~. As part of this contract, Bengt Rydberg performed work that helped to implement handling of radio links. Stefan Buehler's contribution was also supported through the Cluster of Excellence CliSAP 328 (EXC177), Universität Hamburg, funded through the German Science Foundation (DFG).

## References

- Bailey, J. and Kedziora-Chudeczer, L.: Modelling the spectra of planets, brown dwarfs and stars using VSTAR, *Mon. Not. R. Astron. Soc.*, 419, 1913–1929, <https://doi.org/10.1111/j.1365-2966.2011.19845.x>, 2012.
- Battaglia, A., Tanelli, S., Kobayashi, S., Zrnic, D., Hogan, R. J., and Simmer, C.: Multiple-scattering in radar systems: A review, *J. Quant. Spectrosc. Radiat. Transfer*, 111, 917–947, <https://doi.org/10.1016/j.jqsrt.2009.11.024>, 2010.
- Bernstein, L. S., Berk, A., and Sundberg, R. L.: Application of MODTRAN to extra-terrestrial planetary atmospheres, Tech. rep., Spectral Sciences, Inc., Burlington, MA, technical report, 2007.
- Bobryshev, O., Buehler, S. A., John, V. O., Brath, M., and Brogniez, H.: Is there really a closure gap between 183.31 GHz satellite passive microwave and in-situ radiosonde water vapor measurements?, *IEEE T. Geosci. Remote*, 56, 1–7, <https://doi.org/10.1109/TGRS.2017.2786548>, 2018.
- Buehler, S. A., Kuvatov, M., John, V. O., Leiterer, U., and Dier, H.: Comparison of Microwave Satellite Humidity Data and Radiosonde Profiles: A Case Study, *J. Geophys. Res.*, 109, D13103, <https://doi.org/10.1029/2004JD004605>, 2004.
- Buehler, S. A., Eriksson, P., Kuhn, T., von Engeln, A., and Verdes, C.: ARTS, the atmospheric radiative transfer simulator, *J. Quant. Spectrosc. Radiat. Transfer*, 91, 65–93, <https://doi.org/10.1016/j.jqsrt.2004.05.051>, 2005a.
- Buehler, S. A., Verdes, C. L., Tsujimaru, S., Kleinboehl, A., Bremer, H., Sinnhuber, M., and Eriksson, P.: Expected Performance of the SMILES Submillimeter-Wave Limb Sounder compared to Aircraft Data, *Radio Sci.*, 40, RS3016, <https://doi.org/10.1029/2004RS003089>, 2005b.
- Buehler, S. A., Courcoux, N., and John, V. O.: Radiative transfer calculations for a passive microwave satellite sensor: Comparing a fast model and a line-by-line model, *J. Geophys. Res.*, 111, D20304, <https://doi.org/10.1029/2005JD006552>, 2006a.
- Buehler, S. A., von Engeln, A., Brocard, E., John, V. O., Kuhn, T., and Eriksson, P.: Recent developments in the line-by-line modeling of outgoing longwave radiation, *J. Quant. Spectrosc. Radiat. Transfer*, 98, 446–457, <https://doi.org/10.1016/j.jqsrt.2005.11.001>, 2006b.
- Buehler, S. A., John, V. O., Kottayil, A., Milz, M., and Eriksson, P.: Efficient Radiative Transfer Simulations for a Broadband Infrared Radiometer — Combining a Weighted Mean of Representative Frequencies Approach with Frequency Selection by Simulated Annealing, *J. Quant. Spectrosc. Radiat. Transfer*, 111, 602–615, <https://doi.org/10.1016/j.jqsrt.2009.10.018>, 2010.
- Buehler, S. A., Eriksson, P., and Lemke, O.: Absorption lookup tables in the radiative transfer model ARTS, *J. Quant. Spectrosc. Radiat. Transfer*, 112, 1559–1567, <https://doi.org/10.1016/j.jqsrt.2011.03.008>, 2011.
- Cess, R. D.: A radiative transfer model for planetary atmospheres, *J. Quant. Spectrosc. Radiat. Transfer*, 11, 1699–1710, [https://doi.org/10.1016/0022-4073\(71\)90148-8](https://doi.org/10.1016/0022-4073(71)90148-8), 1971.
- Christensen, H. and Veseth, L.: On the high-precision Zeeman effect in O<sub>2</sub> and SO, *J. Molec. Struct.*, 72, 438–444, [https://doi.org/10.1016/0022-2852\(78\)90142-X](https://doi.org/10.1016/0022-2852(78)90142-X), 1978.
- Clough, S. A., Kneizys, F. X., and Davies, R. W.: Line Shape and the Water Vapor Continuum, *Atmos. Res.*, 23, 229–241, [https://doi.org/10.1016/0169-8095\(89\)90020-3](https://doi.org/10.1016/0169-8095(89)90020-3), 1989.
- Clough, S. A., Shephard, M. W., Mlawer, E. J., Delamere, J. S., Iacono, M., Cady-Pereira, K., Boukabara, S., and Brown, P. D.: Atmospheric radiative transfer modeling: a summary of the AER codes, *J. Quant. Spectrosc. Radiat. Transfer*, 91, 233–244, <https://doi.org/10.1016/j.jqsrt.2004.05.058>, 2005.
- Davis, C., Emde, C., and Harwood, R.: A 3D Polarized Reversed Monte Carlo Radiative Transfer Model for mm and sub-mm Passive Remote Sensing in Cloudy Atmospheres, *IEEE T. Geosci. Remote*, 43, 1096–1101, <https://doi.org/10.1109/TGRS.2004.837505>, 2005.

- Davis, C. P., Evans, K. F., Buehler, S. A., Wu, D. L., and Pumphrey, H. C.: 3-D polarised simulations of space-borne passive mm/sub-mm midlatitude cirrus observations: a case study, *Atmos. Chem. Phys.*, 7, 4149–4158, <https://doi.org/10.5194/acp-7-4149-2007>, 2007.
- del Toro Iniesta, J. C.: Introduction to spectropolarimetry, Cambridge university press, ISBN 978-0521818278, 2003.
- Dudhia, A.: The Reference Forward Model (RFM), *J. Quant. Spectrosc. Radiat. Transfer*, 186, 243–253, <https://doi.org/10.1016/j.jqsrt.2016.06.018>, 2017.
- Emde, C., Buehler, S. A., Davis, C., Eriksson, P., Sreerekha, T. R., and Teichmann, C.: A Polarized Discrete Ordinate Scattering Model for Simulations of Limb and Nadir Longwave Measurements in 1D/3D Spherical Atmospheres, *J. Geophys. Res.*, 109, D24207, <https://doi.org/10.1029/2004JD005140>, 2004a.
- Emde, C., Buehler, S. A., Eriksson, P., and Sreerekha, T. R.: The effect of cirrus clouds on microwave limb radiances, *Atmos. Res.*, 72, 383–401, <https://doi.org/10.1016/j.atmosres.2004.03.023>, 2004b.
- Emde, C., Buras-Schnell, R., Kylling, A., Mayer, B., Gasteiger, J., Hamann, U., Kylling, J., Richter, B., Pause, C., Dowling, T., and Bugliaro, L.: The libRadtran software package for radiative transfer calculations (version 2.0.1), *Geosci. Model Dev.*, 9, 1647–1672, <https://doi.org/10.5194/gmd-9-1647-2016>, 2016.
- Encrenaz, T. and Moreno, R.: The microwave spectra of planets, in: AIP Conference Proceedings – EXPERIMENTAL COSMOLOGY AT MILLIMETRE WAVELENGTHS: 2K1BC Workshop, vol. 616, pp. 330–337, <https://doi.org/10.1063/1.1475653>, 2002.
- Eriksson, P., Merino, F., Murtagh, D., Baron, P., Ricaud, P., and de La Noë, J.: Studies for the Odin sub-millimetre radiometer: 1. Radiative transfer and instrument simulation, *Can. J. Phys.*, 80, 321–340, <https://doi.org/10.1139/p02-024>, 2002.
- Eriksson, P., Jiménez, C., Murtagh, D., Elgered, G., Kuhn, T., and Buehler, S.: Measurement of tropospheric/stratospheric transmission at 10–35 GHz for H<sub>2</sub>O retrieval in low Earth orbiting satellite links, *Radio Sci.*, 38, 8069, <https://doi.org/10.1029/2002RS002638>, 2003.
- Eriksson, P., Jiménez, C., and Buehler, S. A.: Qpack, a general tool for instrument simulation and retrieval work, *J. Quant. Spectrosc. Radiat. Transfer*, 91, 47–64, <https://doi.org/10.1016/j.jqsrt.2004.05.050>, 2005.
- Eriksson, P., Ekström, M., Melsheimer, C., and Buehler, S. A.: Efficient forward modelling by matrix representation of sensor responses, *Int. J. Remote Sensing*, 27, 1793–1808, <https://doi.org/10.1080/01431160500447254>, 2006.
- Eriksson, P., Buehler, S. A., Davis, C. P., Emde, C., and Lemke, O.: ARTS, the atmospheric radiative transfer simulator, Version 2, *J. Quant. Spectrosc. Radiat. Transfer*, 112, 1551–1558, <https://doi.org/10.1016/j.jqsrt.2011.03.001>, 2011a.
- Eriksson, P., Buehler, S. A., Emde, C., Sreerekha, T. R., Melsheimer, C., and Lemke, O.: ARTS-2 Theory, ARTS Development Team, regularly updated versions available at <http://www.radiativetransfer.org/docs/>, 2011b.
- Eriksson, P., Buehler, S. A., Emde, C., Sreerekha, T. R., Melsheimer, C., and Lemke, O.: ARTS-2 User Guide, ARTS Development Team, regularly updated versions available at <http://www.radiativetransfer.org/docs/>, 2011c.
- Eriksson, P., Rydberg, B., and Buehler, S. A.: On cloud ice induced absorption and polarisation effects in microwave limb sounding, *Atmos. Meas. Tech.*, 4, 1305–1318, <https://doi.org/10.5194/amt-4-1305-2011>, <http://www.atmos-meas-tech.net/4/1305/2011/>, 2011d.
- Eshleman, V. R., Hinson, D. P., Lindal, G. F., and Tyler, G. L.: Past and future of radio occultation studies of planetary atmospheres, *Adv. Space. Res.*, 7, 29–32, [https://doi.org/10.1016/0273-1177\(87\)90199-2](https://doi.org/10.1016/0273-1177(87)90199-2), 1987.
- Fischer, J., Gamache, R. R., Goldman, A., Rothman, L. S., and Perrin, A.: Total internal partition sums for molecular species in the 2000 edition of the HITRAN database, *J. Quant. Spectrosc. Radiat. Transfer*, 82, 401–412, [https://doi.org/10.1016/S0022-4073\(03\)00166-3](https://doi.org/10.1016/S0022-4073(03)00166-3), 2003.

- Galligani, V. S., Prigent, C., Defer, E., Jimenez, C., Eriksson, P., Pinty, J.-P., and Chaboureaud, J. P.: Meso-scale modelling and radiative transfer simulations of a snowfall event over France at microwaves for passive and active modes and evaluation with satellite observations, *Atmos. Meas. Tech.*, 8, 1605–1616, <https://doi.org/10.5194/amt-8-1605-2015>, 2015.
- Gamache, R. R., Laraia, A. L., and Lamouroux, J.: Half-widths, their temperature dependence, and line shifts for the HDO-CO<sub>2</sub> collision system for applications to CO<sub>2</sub>-rich planetary atmospheres, *Icarus*, 213, 720–730, <https://doi.org/10.1016/j.icarus.2011.03.021>, 2011.
- 5 Gasteiger, J., Emde, C., Mayer, B., Buras, R., Buehler, S. A., and Lemke, O.: Representative wavelengths absorption parameterization applied to satellite channels and spectral bands, *J. Quant. Spectrosc. Radiat. Transfer*, 148, 99–115, <https://doi.org/10.1016/j.jqsrt.2014.06.024>, 2014.
- Gordon, I. E., Rothman, L. S., Hill, C., Kochanov, R. V., Tan, Y., Bernath, P. F., Birk, M., Boudon, V., Campargue, A., Chance, K. V., Drouin, B. J., Flaud, J.-M., Gamache, R. R., Hodges, J. T., Jacquemart, D., Perevalov, V. I., Perrin, A., Shine, K. P., Smith, M.-A. H., Tennyson, J., Toon, G. C., Tran, H., Tyuterev, V. G., Barbe, A., Császár, A. G., Devi, V., Furtenbacher, T., Harrison, J. J., Hartmann, J.-M., Jolly, A., Johnson, T. J., Karman, T., Kleiner, I., Kyuberisa, A. A., Loos, J., Lyulin, O. M., Massie, S. T., Mikhailenko, S. N., Moazzen-Ahmadi, N., Müller, H. S. P., Naumenkom, O. V., Nikitin, A. V., Polyansky, O. L., Reyq, M., Rotger, M., Sharpe, S. W., Sung, K., Starikova, E., Tashkun, S., Vander Auwera, J., Wagnere, G., Wilzewskia, J., Weislo, P., Yu, S., and Zak, E. J.: The HITRAN2016 molecular spectroscopic database, *J. Quant. Spectrosc. Radiat. Transfer*, pp. 1–66, <https://doi.org/10.1016/j.jqsrt.2017.06.038>, 2017.
- 10 Hill, C., Gordon, I. E., Rothman, L. S., and Tennyson, J.: A new relational database structure and online interface for the HITRAN database, *J. Quant. Spectrosc. Radiat. Transfer*, 130, 51–61, <https://doi.org/10.1016/j.jqsrt.2013.04.027>, 2013.
- Hinson, D. P., J., F. M. F. A., Kliore, Schinder, P. J., Twicken, J. D., and Herrera, R. G.: Jupiter’s ionosphere: Results from the First Galileo Radio Occultation Experiment, *Geophys. Res. Lett.*, 24, 2107–2110, <https://doi.org/10.1029/97GL01608>, 1997.
- 20 Jacquinet-Husson, N., Crepeau, L., Armante, R., Boutammine, C., Chédin, A., Scott, N. A., Crevoisier, C., Capelle, V., Boone, C., Poulet-Crovisier, N., Barbe, A., Campargue, A., Chris Benner, D., Benilan, Y., Bézard, B., Boudon, V., Brown, L. R., Coudert, L. H., Coustenis, A., Dana, V., Devi, V. M., Fally, S., Fayt, A., Flaud, J.-M., Goldman, A., Herman, M., Harris, G. J., Jacquemart, D., Jolly, A., Kleiner, I., Kleinböhl, A., Kwabia-Tchana, F., Lavrentieva, N., Lacombe, N., Xu, L.-H., Lyulin, O. M., Mandin, J.-Y., Maki, A., Mikhailenko, S., Müller, C. E., Mishina, T., Moazzen-Ahmadi, N., Müller, H. S. P., Nikitin, A., Orphal, J., Perevalov, V., Perrin, A., Petkie, D. T., Predoi-Cross, A., Rinsland, C. P., Remedios, J. J., Rotger, M., Smith, M. A. H., Sung, K., Tashkun, S., Tennyson, J., Toth, R. A., Vandaele, A.-C., and Vander Auwera, J.: The 2009 edition of the GEISA spectroscopic database, *J. Quant. Spectrosc. Radiat. Transfer*, 112, 2395–2445, <https://doi.org/10.1016/j.jqsrt.2011.06.004>, 2011.
- 25 John, V. O. and Buehler, S. A.: The impact of ozone lines on AMSU-B radiances, *Geophys. Res. Lett.*, 31, L21108, <https://doi.org/10.1029/2004GL021214>, 2004.
- 30 John, V. O., Buehler, S. A., von Engel, A., Eriksson, P., Kuhn, T., Brocard, E., and Koenig-Langlo, G.: Understanding the variability of clear-sky outgoing long-wave radiation based on ship-based temperature and water vapor measurements, *Q. J. R. Meteorol. Soc.*, 132, 2675–2691, <https://doi.org/10.1256/qj.05.70>, 2006.
- Kaplan, L. D.: Inference of Atmospheric Structure from Remote Radiation Measurements, *J. Optical Soc. o. Am.*, 49, 1004–1007, 1959.
- Kasai, Y., Sagawa, H., Kuroda, T., Manabe, T., Ochiai, S., Kikuchi, K., Nishibori, T., Baron, P., Mendrok, J., Hartogh, P., Murtagh, D., Urban, J., von Schéele, F., and Frisk, U.: Overview of the Martian atmospheric submillimetre sounder FIRE, *Planet. Space Sci.*, 63-64, 62–82, <https://doi.org/10.1016/j.pss.2011.10.013>, 2012.
- 35

- Kottayil, A., Buehler, S. A., John, V. O., Miloshevich, L. M., Milz, M., and Holl, G.: On the importance of Vaisala RS92 radiosonde humidity corrections for a better agreement between measured and modeled satellite radiances, *J. Atmos. Oceanic Technol.*, 29, 248–259, <https://doi.org/10.1175/JTECH-D-11-00080.1>, 2012.
- Kursinski, E. R., Hajj, G. A., Leroy, S. S., and Herman, B.: The GPS radio occultation technique, *Terr. Atmos. and Ocean. Sci. J.*, 11, 53–114, [https://doi.org/10.3319/TAO.2000.11.1.53\(COSMIC\)](https://doi.org/10.3319/TAO.2000.11.1.53(COSMIC)), 2000.
- Lammer, H., Kasting, J. F., Chassefière, E., Johnson, R. E., Kulikov, Y. N., and Tian, F.: Atmospheric Escape and Evolution of Terrestrial Planets and Satellites, *Space Sci. Rev.*, 139, 399–436, <https://doi.org/10.1007/s11214-008-9413-5>, 2008.
- Laraia, A. L., Gamache, R. R., Lamouroux, J., Gordon, I. E., and Rothman, L. S.: Total internal partition sums to support planetary remote sensing, *Icarus*, 215, 391–400, <https://doi.org/10.1016/j.icarus.2011.06.004>, 2011.
- 10 Larsson, R.: A note on modelling of the oxygen spectral cross-section in the Atmospheric Radiative Transfer Simulator — Zeeman effect combined with line mixing in Earth’s atmosphere, *Int. J. Remote Sensing*, 35, 5845–5853, <https://doi.org/10.1080/01431161.2014.945002>, 2014.
- Larsson, R., Ramstad, R., Mendrok, J., Buehler, S. A., and Kasai, Y.: A Method for Remote Sensing of Weak Planetary Magnetic Fields: Simulated Application to Mars, *Geophys. Res. Lett.*, 40, 5014–5018, <https://doi.org/10.1002/grl.50964>, 2013.
- 15 Larsson, R., Buehler, S. A., Eriksson, P., and Mendrok, J.: A treatment of the Zeeman effect using Stokes formalism and its implementation in the Atmospheric Radiative Transfer Simulator (ARTS), *J. Quant. Spectrosc. Radiat. Transfer*, 133, 445–453, <https://doi.org/10.1016/j.jqsrt.2013.09.006>, 2014.
- Larsson, R., Milz, M., Rayer, P., Saunders, R., Bell, W., Booton, A., Buehler, S. A., Eriksson, P., and John, V. O.: Modeling the Zeeman effect in high-altitude SSMIS channels for numerical weather prediction profiles: comparing a fast model and a line-by-line model, *Atmos. Meas. Tech.*, <https://doi.org/10.5194/amt-9-841-2016>, 2016.
- 20 Larsson, R., Milz, M., Eriksson, P., Mendrok, J., Kasai, Y., Buehler, S. A., Diéval, C., Brain, D., and Hartogh, P.: Martian magnetism with orbiting sub-millimeter sensor: simulated retrieval system, *Geosci. Instr., Methods and Data Syst.*, 6, 27–37, <https://doi.org/10.5194/gi-6-27-2017>, 2017.
- Le Moal, M. F. and Severin, F.: N<sub>2</sub> and H<sub>2</sub> broadening parameters in the fundamental band of CO, *J. Quant. Spectrosc. Radiat. Transfer*, 35, 145–152, [https://doi.org/10.1016/0022-4073\(86\)90111-1](https://doi.org/10.1016/0022-4073(86)90111-1), 1986.
- 25 Liebe, H. J., Hufford, G. A., and Cotton, M. G.: Propagation modeling of moist air and suspended water/ice particles at frequencies below 1000 GHz, in: AGARD 52nd Specialists’ Meeting of the Electromagnetic Wave Propagation Panel, pp. 3–1–3–10, Palma de Mallorca, Spain, <ftp://ftp.its.blrdoc.gov/pub/mpm93/>, 1993.
- Manabe, S. and Möller, F.: On the radiative equilibrium and heat balance of the atmosphere, *Mon. Weather Rev.*, 89, 503–532, [https://doi.org/10.1175/1520-0493\(1961\)089<0503:OTREAH>2.0.CO;2](https://doi.org/10.1175/1520-0493(1961)089<0503:OTREAH>2.0.CO;2), 1961.
- 30 Mathar, R. J.: Refractive index of humid air in the infrared: model fits, *J. Opt. A: Pure Appl. Opt.*, 9, 470–476, <https://doi.org/10.1088/1464-4258/9/5/008>, 2007.
- Mätzler, C. and Melsheimer, C.: Radiative transfer and microwave radiometry, in: *Thermal Microwave Radiation: Applications for Remote Sensing*, edited by Maetzler, C., vol. 52 of *IET Electromagnetic Waves Series*, chap. 1, pp. 1–23, The Institution of Engineering and Technology, ISBN 0 86341 573 3, 2006.
- 35 Meadows, V. and Crisp, D.: Ground-based near-infrared observations of the Venus nightside: The thermal structure and water abundance near the surface, *J. Geophys. Res.*, 101, 4595–4622, <https://doi.org/10.1029/95JE03567>, 1996.

- Melsheimer, C., Verdes, C., Buehler, S. A., Emde, C., Eriksson, P., Feist, D. G., Ichizawa, S., John, V. O., Kasai, Y., Kopp, G., Koulev, N., Kuhn, T., Lemke, O., Ochiai, S., Schreier, F., Sreerexha, T. R., Suzuki, M., Takahashi, C., Tsujimaru, S., and Urban, J.: Intercomparison of General Purpose Clear Sky Atmospheric Radiative Transfer Models for the Millimeter/Submillimeter Spectral Range, *Radio Sci.*, RS1007, <https://doi.org/10.1029/2004RS003110>, 2005.
- 5 Mendrok, J. and Eriksson, P.: Microwave Propagation Toolbox for Planetary Atmospheres — Final Report (D13a), Tech. rep., ESTEC Contract No 4000104175/11/NL/AF, download at [https://arts.mi.uni-hamburg.de/publications/grouppapers2/mendrok14\\_esa\\_planets\\_fr.pdf](https://arts.mi.uni-hamburg.de/publications/grouppapers2/mendrok14_esa_planets_fr.pdf), 2014.
- Mendrok, J., Eriksson, P., and Perrin, A.: Microwave Propagation Toolbox for Planetary Atmospheres — Technical Note 3 (D5): Propagation model Technical details and expected performance, Tech. rep., ESTEC Contract No 4000104175/11/NL/AF, 2014.
- 10 Mlawer, E. J., Payne, V. H., Moncet, J.-L., Delamere, J. S., Alvarado, M. J., and Tobin, D. C.: Development and recent evaluation of the MT\_CKD model of continuum absorption, *Phil. Trans. R. Soc. A*, 370, 2520–2556, <https://doi.org/10.1098/rsta.2011.0295>, 2012.
- Mobley, C. D.: *Light and Water: Radiative Transfer in Natural Waters*, Academic Press, ISBN 978-0125027502, 1994.
- Navas-Guzmán, F., Kämpfer, N., Murk, A., Larsson, R., Buehler, S. A., and Eriksson, P.: Zeeman effect in atmospheric O<sub>2</sub> measured by ground-based microwave radiometry, *Atmos. Meas. Tech.*, pp. 1863–1874, <https://doi.org/10.5194/amt-8-1863-2015>, 2015.
- 15 Newell, A. C. and Baird, R. C.: Absolute Determination of Refractive Indices of Gases at 47.7 Gigahertz, *J. Appl. Phys.*, 36, <https://doi.org/10.1063/1.1713942>, 1965.
- Nilsson, T. and Elgered, G.: Long-term trends in the atmospheric water vapor content estimated from ground-based GPS data, *J. Geophys. Res.*, 113, D19101, <https://doi.org/10.1029/2008JD010110>, 2008.
- Oschlinskiok, J., Häusler, B., Pätzold, M., Tyler, G. L., Bird, M. K., Tellmann, S., Remus, S., and Andert, T.: Microwave absorptivity by sulfuric acid in the Venus atmosphere: First results from the Venus Express Radio Science experiment VeRa, *Icarus*, 221, 940–948, <https://doi.org/10.1016/j.icarus.2012.09.029>, 2012.
- Owen, T. and Encrenaz, T.: Element abundances and isotope ratios in the giant planets and Titan, *Space Sci. Rev.*, 106, 121–138, <https://doi.org/10.1023/A:1024633603624>, 2003.
- Perrin, A., Puzzarini, C., Colmont, J.-M., Verdes, C., Wlodarczak, G., Cazzoli, G., Buehler, S., Flaud, J.-M., and Demaison, J.: Molecular line parameters for the MASTER (Millimeter wave Acquisitions for Stratosphere/Troposphere Exchange Research) database, *J. Atmos. Chem.*, 50, 161–205, <https://doi.org/10.1007/s10874-005-7185-9>, 2005.
- Phillips, N. A.: The general circulation of the atmosphere: A numerical experiment, *Q. J. R. Meteorol. Soc.*, 82, 123–164, <https://doi.org/10.1002/qj.49708235202>, 1956.
- Pickett, H., Poynter, R. L., Cohen, E. A., Delitsky, M. L., Pearson, J. C., and Müller, H. S. P.: Submillimeter, millimeter, and microwave spectral line catalog, *J. Quant. Spectrosc. Radiat. Transfer*, 60, 883–890, [https://doi.org/10.1016/S0022-4073\(98\)00091-0](https://doi.org/10.1016/S0022-4073(98)00091-0), 1998.
- 30 Pickett, H. M.: Effects of velocity averaging on the shapes of absorption lines, *J. Chem. Phys.*, pp. 919–928, 1980.
- Pincus, R., Mlawer, E. J., Oreopoulos, L., Ackerman, A. S., Baek, S., Brath, M., Buehler, S. A., Cady-Pereira, K. E., Cole, J. N. S., Dufresne, J.-L., Kelley, M., Li, J., Manners, J., Paynter, D. J., Roehrig, R., Sekiguchi, M., and Schwarzkopf, D. M.: Radiative flux and forcing parameterization error in aerosol-free clear skies, *Geophys. Res. Lett.*, 42, 5485–5492, <https://doi.org/10.1002/2015GL064291>, 2015.
- 35 Plass, G. N.: The influence of the 15 $\mu$  carbon-dioxide band on the atmospheric infra-red cooling rate, *Q. J. R. Meteorol. Soc.*, 82, 310–324, <https://doi.org/10.1002/qj.49708235307>, 1956.
- Pumphrey, H. C. and Buehler, S. A.: Instrumental and Spectral Parameters: Their Effect on and Measurement by Microwave Limb Sounding of the Atmosphere, *J. Quant. Spectrosc. Radiat. Transfer*, 64, 421–437, 2000.

- Richard, C., Gordon, I. E., Rothman, L. S., Abel, M., Frommhold, L., Gustafsson, M., Hartmann, J.-M., Hermans, C., Lafferty, W. J., Orton, G. S., Smith, K., and Tran, H.: New section of the HITRAN database: Collision-induced absorption (CIA), *J. Quant. Spectrosc. Radiat. Transfer*, 113, 1276–1285, <https://doi.org/10.1016/j.jqsrt.2011.11.004>, 2012.
- Rodgers, C. D., ed.: *Inverse Methods for Atmospheric Sounding: Theory and Practice*, World Scientific Publishing, ISBN-10 981022740X, 5 2000.
- Rosenkranz, P. W.: Absorption of microwaves by atmospheric gases, in: *Atmospheric remote sensing by microwave radiometry*, edited by Janssen, M. A., pp. 37–90, John Wiley and Sons, Inc., ISBN 0-471-62891-3, [ftp://mesa.mit.edu/phil/lbl\\_rt](ftp://mesa.mit.edu/phil/lbl_rt), 1993.
- Rosenkranz, P. W.: Water vapor microwave continuum absorption: A comparison of measurements and models, *Radio Sci.*, 33, 919–928, (correction in 34, 1025, 1999), [ftp://mesa.mit.edu/phil/lbl\\_rt](ftp://mesa.mit.edu/phil/lbl_rt), 1998.
- 10 Rothman, L. S., Gordon, I. E., Barbe, A., Benner, D. C., Bernath, P. F., Birk, M., Boudon, V., Brown, L. R., Campargue, A., Champion, J.-P., Chance, K., Coudert, L. H., Dana, V., Devi, V. M., Fally, S., Flaud, J.-M., Gamache, R. R., Goldman, A., Jacquemart, D., Kleiner, I., Lacombe, N., Lafferty, W. J., Mandin, J.-Y., Massie, S. T., Mikhailenko, S. N., Miller, C. E., Moazzen-Ahmadi, N., Naumenko, O. V., Nikitin, A. V., Orphal, J., Perevalov, V. I., Perrin, A., Predoi-Cross, A., Rinsland, C. P., Rotger, M., Simeckova, M., Smith, M. A. H., Sung, K., Tashkun, S. A., Tennyson, J., Toth, R. A., Vandaele, A. C., and Auwera, J. V.: The HITRAN 2008 molecular spectroscopic database, 15 *J. Quant. Spectrosc. Radiat. Transfer*, 110, 533–572, <https://doi.org/10.1016/j.jqsrt.2009.02.013>, 2009.
- Rothman, L. S., Gordon, I. E., Babikov, Y., Barbe, A., Benner, D. C., Bernath, P. F., Birk, M., Bizzocchi, L., Boudon, V., Brown, L. R., Campargue, A., Chance, K., Cohen, E. A., Coudert, L. H., Devi, V. M., Drouin, B. J., Fayt, A., Flaud, J.-M., Gamache, R. R., Harrison, J. J., Hartmann, J.-M., Hill, C., Hodges, J. T., Jacquemart, D., Jolly, A., Lamouroux, J., Le Roy, R. J., Li, G., Long, D. A., Lyulin, O. M., Mackie, C. J., Massie, S. T., Mikhailenko, S., Müller, H. S. P., Naumenko, O. V., Nikitin, A. V., Orphal, J., Perevalov, 20 V., Perrin, A., Polovtseva, E. R., Richard, C., Smith, M. A. H., Starikova, E., Sung, K., Tashkun, S., Tennyson, J., Toon, G. C., Tyuterev, V. G., and Wagner, G.: The HITRAN2012 molecular spectroscopic database, *J. Quant. Spectrosc. Radiat. Transfer*, 130, 4–50, <https://doi.org/10.1016/j.jqsrt.2013.07.002>, 2013.
- Rüfenacht, R., Murk, A., Kämpfer, N., Eriksson, P., and Buehler, S. A.: Middle-atmospheric zonal and meridional wind profiles from polar, tropical and midlatitudes with the ground-based microwave Doppler wind radiometer WIRA, *Atmos. Meas. Tech.*, 7, 4491–4505, 25 <https://doi.org/10.5194/amt-7-4491-2014>, 2014.
- Rybicki, G. B. and Lightman, A. P.: *Radiative Processes in Astrophysics*, John Wiley and Sons, Inc., USA, ISBN 978-0-471-82759-7, 1979.
- Rydberg, B., Eriksson, P., and Buehler, S. A.: Prediction of cloud ice signatures in sub-mm emission spectra by means of ground-based radar and in-situ microphysical data, *Q. J. R. Meteorol. Soc.*, 133, 151–162, <https://doi.org/10.1002/qj.151>, 2007.
- Rydberg, B., Eriksson, P., Buehler, S. A., and Murtagh, D. P.: Non-Gaussian Bayesian retrieval of tropical upper tropospheric cloud ice and 30 water vapour from Odin-SMR measurements, *Atmos. Meas. Tech.*, 2, 621–637, <https://doi.org/10.5194/amt-2-621-2009>, 2009.
- Schreier, F., Garcia, S. G., Hedelt, P., Hess, M., Mendrok, J., Vasquez, M., and Xu, J.: GARLIC - A general purpose atmospheric radiative transfer line-by-line infrared-microwave code: Implementation and evaluation, *J. Quant. Spectrosc. Radiat. Transfer*, 137, 29–50, <https://doi.org/10.1016/j.jqsrt.2013.11.018>, 2014.
- Schreier, F., Milz, M., Buehler, S. A., and von Clarmann, T.: Intercomparison of three microwave/infrared high resolution line-by-line 35 radiative transfer codes, *J. Quant. Spectrosc. Radiat. Transfer*, <https://doi.org/10.1016/j.jqsrt.2018.02.032>, in press, 2018.
- Sreerekha, T. R., Buehler, S. A., O’Keefe, U., Doherty, A., Emde, C., and John, V. O.: A strong ice cloud event as seen by a microwave satellite sensor: Simulations and Observations, *J. Quant. Spectrosc. Radiat. Transfer*, 109, 1705–1718, <https://doi.org/10.1016/j.jqsrt.2007.12.023>, 2008.

- Stamnes, K., Tsay, S.-C., Wiscombe, W., and Jayaweera, K.: Numerically stable algorithm for discrete-ordinate-method radiative transfer in multiple scattering and emitting layered media, *Appl. Opt.*, 27, 2502–2509, <https://doi.org/10.1364/AO.27.002502>, 1988.
- Stratton, A. J.: Optical and Radio Refraction on Venus, *J. Atmos. Sci.*, 25, 666–667, [https://doi.org/10.1175/1520-0469\(1968\)025<0666:OARROV>2.0.CO;2](https://doi.org/10.1175/1520-0469(1968)025<0666:OARROV>2.0.CO;2), 1968.
- 5 Thayer, G. D.: An improved equation for the radio refractive index of air, *Radio Sci.*, 9, 803–807, 1974.
- Turbet, M. and Tran, H.: Comment on “Radiative Transfer in CO<sub>2</sub>-Rich Atmospheres: 1. Collisional Line Mixing Implies a Colder Early Mars”, *J. Geophys. Res.: Plan.*, 122, 2362–2365, <https://doi.org/10.1002/2017JE005373>, 2017.
- Ulaby, F. T., Long, D. G., Blackwell, W. J., Elachi, C., Fung, A. K., Ruf, C., Sarabandi, K., Zebker, H. A., and Van Zyl, J.: *Microwave radar and radiometric remote sensing*, vol. 4, University of Michigan Press Ann Arbor, 2014.
- 10 Urban, J., Dassas, K., Forget, F., and Ricaud, P.: Retrieval of vertical constituents and temperature profiles from passive submillimeter wave limb observations of the Martian atmosphere: a feasibility study, *Appl. Opt.*, 44, 2438–2455, 2005.
- Varanasi, P.: Measurement of line widths of CO of planetary interest at low temperatures, *J. Quant. Spectrosc. Radiat. Transfer*, 15, 191–196, [https://doi.org/10.1016/0022-4073\(75\)90017-5](https://doi.org/10.1016/0022-4073(75)90017-5), 1975.
- Vasquez, M., Schreier, F., García, S. G., Kitzmann, D., Patzer, B., Rauer, H., and Trautmann, T.: Infrared radiative transfer in atmospheres of Earth-like planets around F, G, K, and M stars - I. Clear-sky thermal emission spectra and weighting functions, *A&A*, 549, A26–1–13, <https://doi.org/10.1051/0004-6361/201219898>, 2013a.
- 15 Vasquez, M., Schreier, F., García, S. G., Kitzmann, D., Patzer, B., Rauer, H., and Trautmann, T.: Infrared radiative transfer in atmospheres of Earth-like planets around F, G, K, and M stars. II. Thermal emission spectra influenced by clouds, *A&A*, 557, A46, <https://doi.org/10.1051/0004-6361/201220566>, 2013b.
- 20 Verdes, C. L., Buehler, S. A., Perrin, A., Flaud, J.-M., Demaison, J., Wlodarczak, G., Colmont, J.-M., Cazzoli, G., and Puzzarini, C.: A Sensitivity Study on Spectroscopic Parameter Accuracies for a mm/sub-mm Limb Sounder Instrument, *J. Molec. Spectro.*, 229, 266–275, <https://doi.org/10.1016/j.jms.2004.09.014>, 2005.
- Veseth, L.: Relativistic Corrections to the Zeeman Effect in Diatomic Molecules, *J. Molec. Struct.*, 66, 259–271, [https://doi.org/10.1016/0022-2852\(77\)90216-8](https://doi.org/10.1016/0022-2852(77)90216-8), 1977.
- 25 Zeeman, P.: On the Influence of Magnetism on the Nature of the Light Emitted by a Substance, *Astrophys. J.*, 5, 332–347, <https://doi.org/10.1086/140355>, 1897.